9-1-2007

Uniaxial Tensile Testing of Superelastic CuAlBe Wires at Cold Temperatures

Y. Zhang

J. Camilleri

S. Zhu

LEHIGH
UNIVERSITY

Uniaxial Tensile Testing of Superelastic CuAlBe Wires at Cold Temperatures

by

Yunfeng Zhang

Joseph Camilleri

Songye Zhu

ATLSS Report No. 07-08

September 2007

ATLSS is a National Center for Engineering Research on Advanced Technology for Large Structural Systems

117 ATLSS Drive
Bethlehem, PA 18015-4729

Phone: (610)758-3525
Fax: (610)758-5902

www.atlss.lehigh.edu
Email: inatl@lehigh.edu

Cyclic Load Testing of Superelastic CuAlBe Wires at Cold Temperatures

by

Yunfeng Zhang
Associate Professor
yuz8@lehigh.edu

Joseph Camilleri
REU Student

Songye Zhu
Graduate Research Assistant

ATLSS Report No. 07-08

September 2007

ATLSS is a National Center for Engineering Research on Advanced Technology for Large Structural Systems

117 ATLSS Drive
Bethlehem, PA 18015-4729

Phone: (610)758-3525
Fax: (610)758-5902

www.atlss.lehigh.edu
Email: inatl@lehigh.edu

Abstract

This report presents the results of an experimental characterization of the mechanical properties of superelastic copper-aluminum-beryllium (Cu-Al-Be) alloy wires at cold temperatures. This research is motivated by the recent use of shape memory alloys for bridge restrainer, which could be subject to harsh winter conditions, especially in cold regions. Bridge restrainers made of superelastic Cu-Al-Be wire strands are expected to be used for protecting bridge decks from excessive displacement when subjected to strong earthquakes. Using a temperature chamber, superelastic Cu-Al-Be wires with a diameter of 1.5 mm were tested under uniaxial cyclic loading at various loading rates and cold temperatures. The test results from 20°C to -50°C demonstrate that Cu-Al-Be exhibits superelastic behavior at cold temperatures down to -85°C. It is also found that with decreasing temperatures the transformation stress is reduced while its fatigue life increases under cyclic testing.

Table of Contents

Chapter 1

Introduction

Historical strong earthquakes have demonstrated that unseating of deck superstructures is one of the primary causes of bridge collapse. This catastrophic result occurs when the seismically induced relative displacement between the deck and the supporting substructure exceeds the available seat width. The collapse of bridges due to deck unseating during recent earthquakes 1989 Loma Prieta Earthquake, 1994 Northridge earthquake, 1999 Chi Chi earthquake has emphasized the need to implement modern seismic protection technologies (Dicleli and Bruneau 1995; Saiidi et al 2001, Hsu and Fu 2004). To reduce the likelihood of collapse due to unseating, a variety of unseating prevention devices have been developed because they are less expensive than substructure retrofits and require fewer service interruptions. For example, steel cable or-rod restrainers are often used between the girders and the piers of the bridge.

The traditional steel cable restrainers or rods used have several limitations such as small elastic strain range and limited ductility capacity. To address these limitations, superelastic Nitinol cables have been used for unseating prevention devices and research has shown that Nitinol restrainers are generally more effective than steel cable restrainers in reducing the relative displacements (Andrawes and DesRoches 2005). Due to the superelastic behavior of Nitinol, the use of superelastic Nitinol restrainers in bridges can reduce the movement of the bridge deck as well as dissipate the seismic energy through phase transformation from austenite to martensite. Superelastic Nitinol restrainer can

recover its shape up to 8% strain and has a very high fatigue life (over two thousands loading cycles at 8% strain based on the writers' test results). However, Nitinol is fairly sensitive to temperature changes with respect to its hysteretic cycle and will lose its superelastic behavior at cold temperatures. Figure 1 shows that at 0°C Nitinol starts to loose its superelastic ability and at -25°C Nitinol has completely lost all of its superelastic ability. According to ASTM 709 bridge steel specification (2005), the lowest service temperature (i.e., for AASHTO Zone 3) in bridge application is set to be -51°C. Therefore, the use of Nitinol bridge restrainers will be limited at cold temperatures, such as in the winter climates of places like Missouri and Canada.

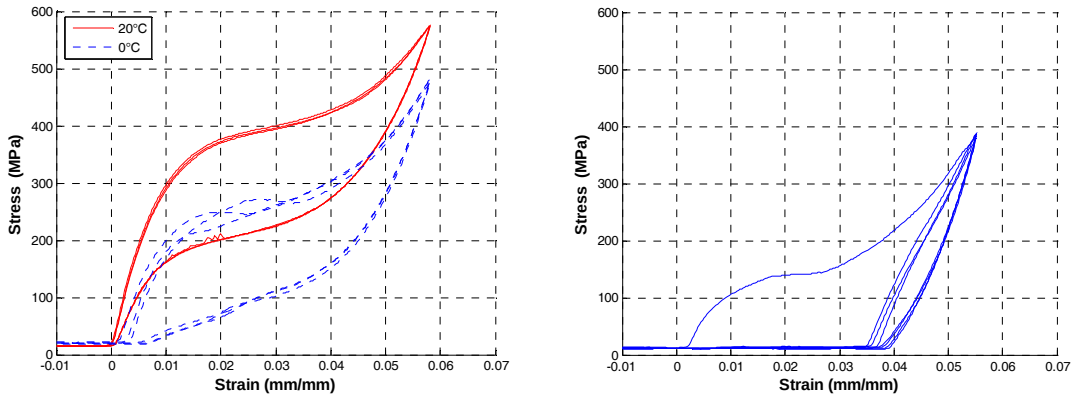

Figure 1. Experimental stress-strain curve of Nitinol wire at various temperatures: (a) 20°C and 0°C, (b) -25°C (Superelastic effect is lost)

Recently, copper-based alloys have attracted certain attention for seismic applications because they are less expensive and easier to machine. Casciati and Faravelli (2004), Cerda *et al* (2006), and Isalgue *et al* (2006) studied Cu-Al-Be alloy towards its use as passive damping device for seismic response control of civil engineering structures.

Cerda *et al* (2006) examined the seismic response of scaled 3-story steel frame structure equipped with Cu-Al-Be bracings through shaking table test. It was found that the inclusion of Cu-Al-Be bracings increased the damping ratio from 0.59% in the bare structure to 5.95% in the braced structure and reduced peak acceleration and peak displacements by nearly 60%. Isalgue *et al* (2006) did a simulation study, in which Cu-Al-Be alloy was used as diagonal braces in a two-story frame structure. Their result shows that using Cu-Al-Be bracing can reduce the vibration response of the frame structure by at least a factor of 2 under the action of earthquakes. However, the most noteworthy property of Cu-Al-Be alloy is its very wide operating temperature range from -80°C to over 100°C for retaining its superelastic behavior according to the writers' experimental results. This property distinguishes Cu-Al-Be from other known shape memory alloys and has a great potential to be applied as damping devices in outdoor environment, even at cold regions.

Motivated by its potential outdoor application such as bridge unseating prevention device in cold regions, this report presents the results of the evaluation of Cu-Al-Be alloy under uniaxial cyclic loading. In this study, a series of experiments were conducted on superelastic Cu-Al-Be wires at various temperatures and loading rates. The main objective was to evaluate the effect of cold temperature and loading rates on the superelastic behavior of Cu-Al-Be alloy.

Chapter 2

Test Sample Preparation

For this experimental study, superelastic Cu-Al-Be alloy wires with a 1.4-mm diameter were acquired from a French manufacturer. The materials studied are Cu-Al-Be polycrystalline SMAs. The superelastic polycrystalline Cu-Al-Be wire used in this study was cold drawn. The alloy has its chemical composition in weight as: Al = 11.7%; Be = 0.62%; Cu = 87.68%. The test conducted by the producer gave the following results for the transformation temperatures: A_s = -105°C, A_f = -65°C. The superelasticity of these alloys persists until 180°C and thus for normal outdoor operating condition the Cu-Al-Be alloy will exhibit superelastic behavior.

When initially purchased, the as-drawn Cu-Al-Be SMA wires exhibit no superelastic effect. In order for these wires to exhibit these properties a heat treatment process is necessary. Due to size limitations on the kiln being used to heat treat the wires, two separate batches of Cu-Al-Be wires were heat treated, denoted as batch 1 and batch 2. Thermal treatment of the Cu-Al-Be wire samples includes heating for 30 or 20 minutes at 750°C, water quenching to the ambient temperature of 24°C by immersion in water for about 10 seconds. Batch 1 received 30 minutes of heating while batch 2 received 20 minutes. The heat treatment process had a quite significant effect on the stress-strain relationships of Cu-Al-Be wires, as shown in Figure 2. Wires from batch 1 tend to have lower energy dissipating capacity than batch 2 wires. It is also observed after cyclic testing was completed that under the 1-Hz loading frequency the Cu-Al-Be wires from

batch 1 consistently had a better fatigue life than batch 2 wires. At every temperature the number of cycles required to fracture of the wire samples was greater for batch 1. This shows that batch 1 is tougher and can undergo more fatigue. A comparison of average fatigue life of Cu-Al-Be wires from batch 1 and batch 2 is shown in Table 1. Due to these differences, each test combination in the test program used three Cu-Al-Be wires from batch 1 and two wires from batch 2.

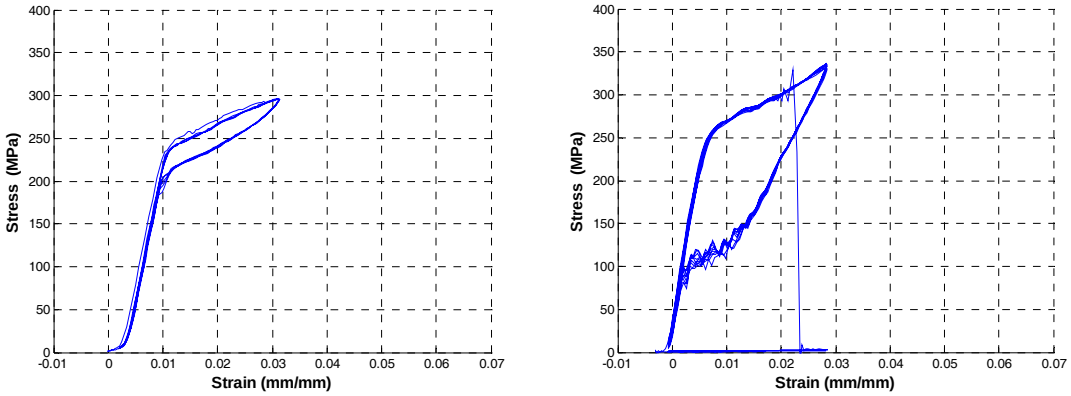

(a) (b)

Figure 2. Effect of different heat treat processes on Cu-Al-Be wire at 23°C: (a) Batch 1; (b) Batch 2

Preliminary testing was done in order to train the superelastic Cu-Al-Be wires before formal testing. The heat-treated Cu-Al-Be wires were cut into pieces with a 305 mm (12 inch) length, which were tested under cyclic tension load using a test set-up shown in Figure 3. Figure 3 shows the changes in the hysteretic behavior of Cu-Al-Be wires under cyclic loading for the first ten load cycles. It is seen that at a strain rate of 0.06 sec^{-1} visible changes including strain shift at zero stress, decrease of 'yield' stress and hysteresis area occur in the first ten load cycles. After the first ten load cycles, the hysteretic behavior of Cu-Al-Be wires stabilizes to a steady-state hysteresis loop. Usually the first one to four load cycles exhibited some residual strain, but after that the Cu-Al-Be

specimen would almost completely re-center itself to the original length, as shown in Figure 3. Training of superelastic Cu-Al-Be wires thus proved to be necessary before formal testing to stabilize the hysteresis and eliminate residual strain. In the preliminary test, each of the Cu-Al-Be wire specimens tested were first trained for 5 cycles at a loading frequency of 1 Hz before formal testing.

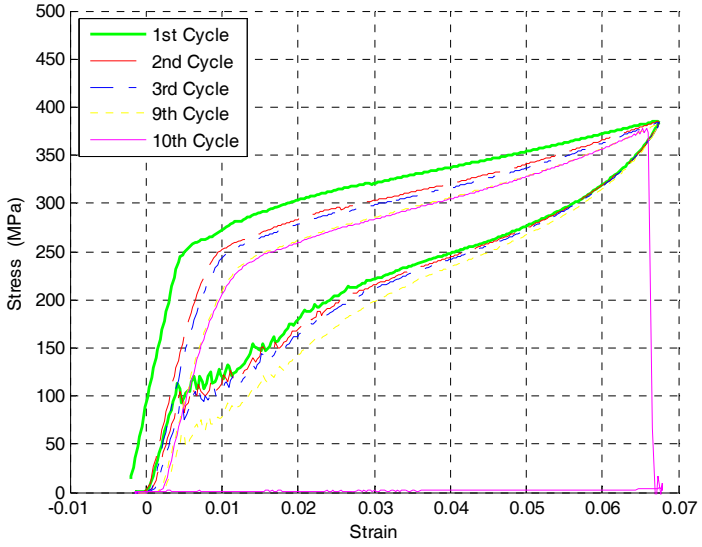

Figure 3. Training effect of CuAlBe wires

Table 1. Effect of different heat treatment on Cu-Al-Be wire

Temperature (ºC)	Average # of Cycles to Fracture	
	Batch 1	Batch 2
23	54.8	13.3
0	38.3	38.0
-25	96.0	43.0
-50	101.0	51.5

Chapter 3

Uniaxial Tensile Test

3.1 Test Program

In order to evaluate the mechanical properties of superelastic Cu-Al-Be alloys at cold temperature, cyclic loading of Cu-Al-Be wires need to be performed at various loading rates and test temperatures. The Cu-Al-Be wire samples were tested using an MTS universal hydraulic testing machine at a variety of temperatures, and the test length of the Cu-Al-Be wire specimens was equal to 305 mm (10 inch). The Cu-Al-Be wires were cyclically loaded under 3% strain cycles. Cyclic tension tests were conducted under displacement control with constant strain rate. The test matrix for this experimental study is given in Table 2. The tests were completed using 7 wires at 0.02 Hz and 7 wires at 1 Hz, 3 being from batch and 2 and 4 from batch 1. Cold tests were conducted in the same manner as the room temperature tests, except only 3 wires from batch 1 and 2 wires from batch 2 were tested for each frequency and each temperature. In total 30 cold temperature tests were completed.

Table 2. Test matrix for Cu-Al-Be wires

Temperature (°C)	**Loading Frequency**	
	0.02 Hz ($\dot{\varepsilon} = 0.0012\ s^{-1}$)	1 Hz ($\dot{\varepsilon} = 0.06\ s^{-1}$)
23	7 (4 B1, 3 B2)	7 (4 B1, 3 B2)
0	5 (3 B1, 2 B2)	5 (3 B1, 2 B2)
-25	5 (3 B1, 2 B2)	5 (3 B1, 2 B2)
-50	5 (3 B1, 2 B2)	5 (3 B1, 2 B2)

Note: B1 = Batch 1; B2 Batch 2

Two loading frequencies - 0.02 Hz and 2 Hz at 3% strain cycles, which corresponds to a strain rate $\dot{\varepsilon}$ of 0.0012 sec^{-1} or 0.06 sec^{-1} respectively are adopted in the formal test study. Cold temperature test is an integral part of this study. As seen in Table 2, the Cu-Al-Be wire samples were tested at 23ºC, 0ºC -25ºC and -50ºC respectively. A complete list of tested wires is given in Table 4. A temperature-controlled test chamber as shown in Figures 3 and 4 was utilized to maintain the specified low temperature, which measures 343-mm x 292-mm x 394-mm (13.5-inch x 11.5-inch x15.5-inch) and fits inside the universal testing machine being used. The temperature chamber is in-house made and is able to maintain a temperature of at least -100ºC. A temperature process controller was configured to activate a solenoid valve for liquid nitrogen tank to maintain the cryogenic test condition. At this point the temperature would fluctuate only about +/- 3ºC. The test temperature was monitored using a set of insulated thermocouples placed inside the temperature chamber.

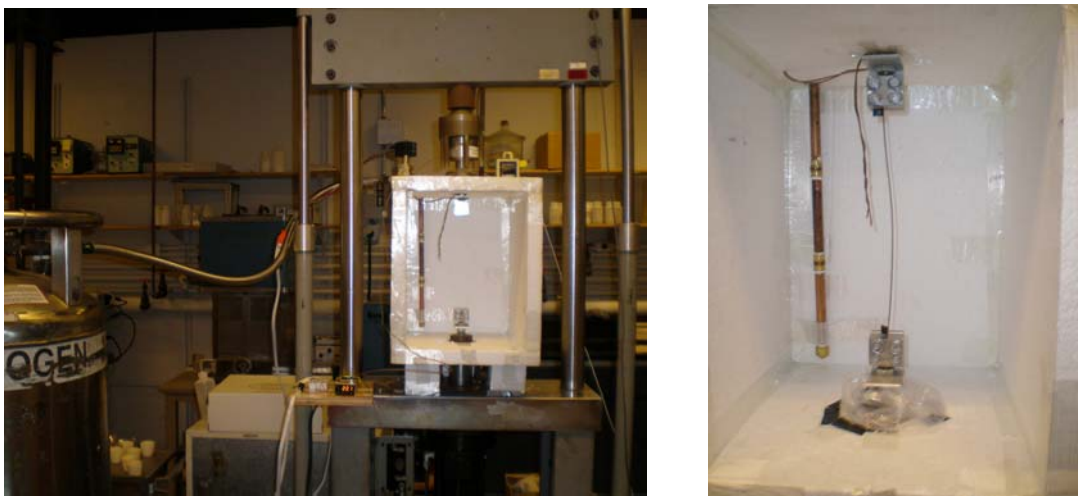

Figure 3. Setup for cold temperature test

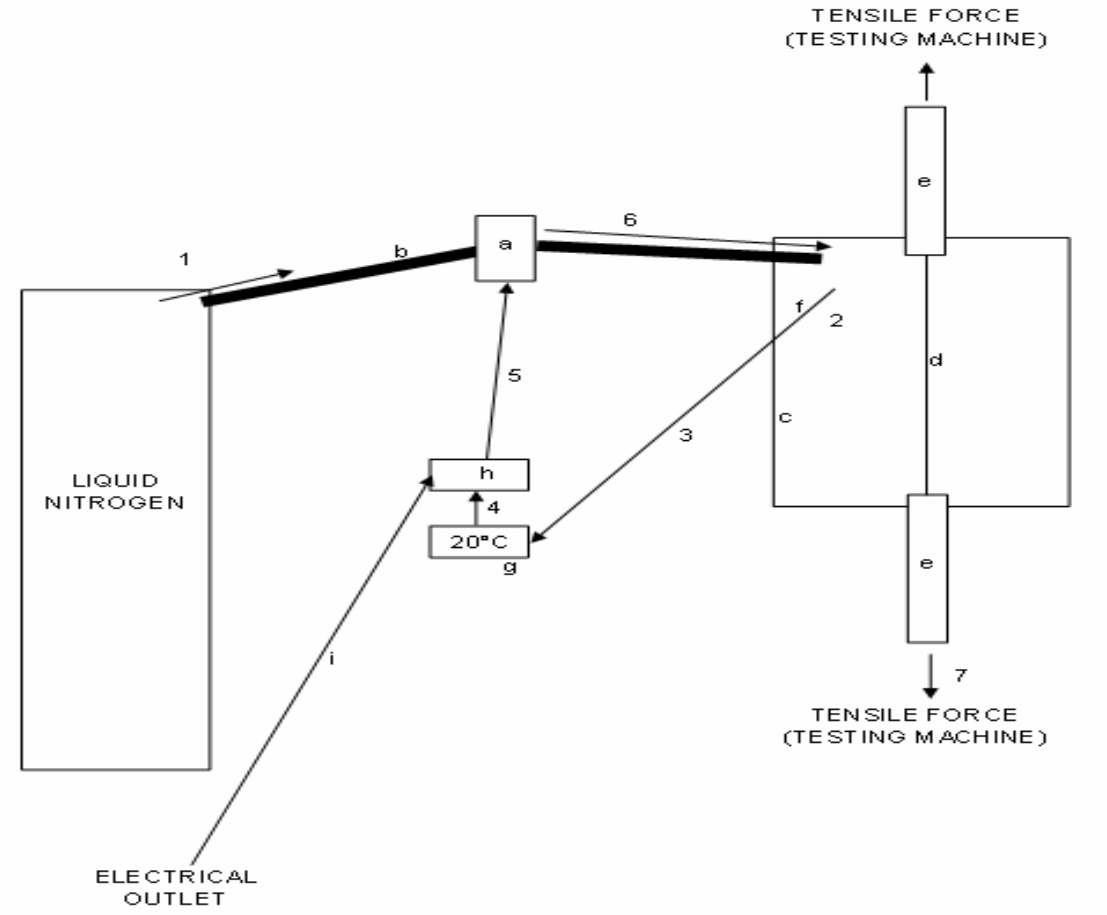

Figure 4. Schematics of test-setup components

Legend of Figure 4

a. Normally closed solenoid valve
b. Cryogenic hose
c. 1½" thick polystyrene foam temperature chamber
d. 1.4mm diameter CuAlBe SMA wire
e. Instron testing machine
f. Type "k" insulated thermocouple
g. Temperature process controller
h. Solid state relay
i. Electrical extension cord

1. Liquid nitrogen valve is opened, cold liquid nitrogen passes through cryogenic hose and is stopped by the normally closed solenoid valve
2. Thermocouple reads temperature inside box
3. Temperature reading is sent to the temperature process controller
4. If temperature is above set point (-50°C) the temperature process controller sends a signal to the solid state relay which activates
5. Upon activation of the solid state relay the extension cord is also activated which then activates and opens the solenoid valve
6. Cold nitrogen which is now in the gas phase rushes into the temperature chamber

3.2 Result and Discussion

Figures 5 and 6 plot the representative stress-strain curves for the superelastic Cu-Al-Be wires under uniaxial cyclic test. Each curve in these figures corresponds a particular combination of test temperatures (23ºC, 0ºC -25ºC, -50ºC), strain rate (0.0012 sec^{-1} or 0.06 sec^{-1}), and heat treatment (batch 1 or batch 2). The effects of test temperature, strain rate, and heat treatment on key hysteresis parameters of these Cu-Al-Be wires including transformation stress (i.e., 'yield' stress at the upper transformation plateau), equivalent damping ratio, elastic modulus, and upper transformation plateau slope are shown in Figures 7 to 10. "Yields" is put into quotations because the Cu-Al-Be SMA is not really yielding as an ordinary alloy like steel would. This "yield" is due to the solid state phase transformation from austenite to martensite. At the yield point this phase transformation begins and the percentage of martensite in the material begins to increase with load. While unloading the opposite occurs. A complete list of such effects on transformation stress, initial stiffness, and transformation plateau stiffness is given in Table 5.

For these two batches, similar observations regarding the variation of transformation stress can be made. The first thing that stands out when studying the cold tests is that Cu-Al-Be "yields" at a lower stress level. Therefore due to the relatively flat slope of the upper plateau, specimens at cold temperatures undergo less stress at equal strains. It is further seen in Figure 7 that the transformation stress of the Cu-Al-Be wires being tested increases almost linearly with temperature. The transformation stresses of the Cu-Al-Be wires from two different batches seem to be very close to each other at each test temperature and follow a similar temperature variation pattern. Higher strain rate appear to lead to slightly increased transformation stress level, especially at lower temperatures.

This is probably due to a self-heating phenomenon in the loading process. In general, the loading path is accompanied with a rise in wire temperature while the unloading path is associated with a temperature drop. In cycling loading tests with higher loading rates, the heat generated during loading may not be dissipated as quickly as it is created and thus the transformation plateau shifts upwards.

Figures 8 and 9 show the energy dissipated per load cycle and equivalent viscous damping ratio of the Cu-Al-Be wires respectively. The energy dissipated per cycle is normalized to a 3% strain amplitude since it is seen from Figures 5 and 6 that the peak strain for the Cu-Al-Be tested at different temperatures are not same (due to thermal contraction of Cu-Al-Be wires at cold temperatures). To measure the energy dissipating capacity of the Cu-Al-Be wires, a quantitative index termed equivalent viscous damping ratio is employed, as defined below,

$$\zeta_{eq} = \frac{E_D}{4\pi \cdot E_{So}} \tag{1}$$

where E_D is the energy dissipated in one load cycle, i.e., the area enclosed by the hysteresis loop, and E_{So} is the maximum strain energy in one load cycle. It is seen in Figure 8 that for batch 1, the energy dissipation per load cycle does not change with temperature while for batch 2 the energy dissipation at room temperature is considerably greater than that at cold temperatures. For batch 1, the loading rate seems to have no effect on the energy dissipation capacity of Cu-Al-Be wires. For batch 2, at room temperature, higher loading rate leads to increased energy dissipation while at cold temperatures, loading rate has very little or no effect on the energy dissipation capacity of Cu-Al-Be wires. In Figure 9, it is seen that the equivalent damping ratio of Cu-Al-Be wires slightly decreases with temperature from -50°C to 0°C. This may be explained by

the lower transformation stress value at colder temperatures which reduce the value of E_{So} in Equation 1.

Figure 10 shows the elastic modulus of the Cu-Al-Be wires at different test temperatures and load ratings. The elastic modulus of batch 2 wires is slightly higher than that of batch 1 wires. The average value of the elastic modulus for batch 1 and batch 2 wires are 33.9 GPa and 36.1 GPa respectively. These values are slightly lower than that of austenite NiTi alloy which has a modulus of elastic equal to 40.9 GPa from room temperature test. No significant variation pattern of the elastic modulus with respect to temperature and loading rates can be made.

Figure 11 shows the upper transformation plateau slope of the Cu-Al-Be wires being tested. It is seen that the slope values of the batch 2 wires are generally higher than those of the batch 1 wires. Loading rate seems to have very little effect on the upper transformation plateau slope of the Cu-Al-Be wires. It is also seen that with the increase of test temperature the value of upper transformation plateau slope decreases.

Figures 12 to 14 show a scanning electronic microscope (SEM) picture of the fracture surface of the Cu-Al-Be wires failed under cyclic loading (1 Hz) at 0°C, -25°C, and -50°C respectively. Figures 15-(a) and 15-(b) shows a zoomed view of local fracture surface of the Cu-Al-Be wire corresponding to Figure 13 and 14 respectively. It is seen that the fracture surface involved certain degree of plastic deformation.

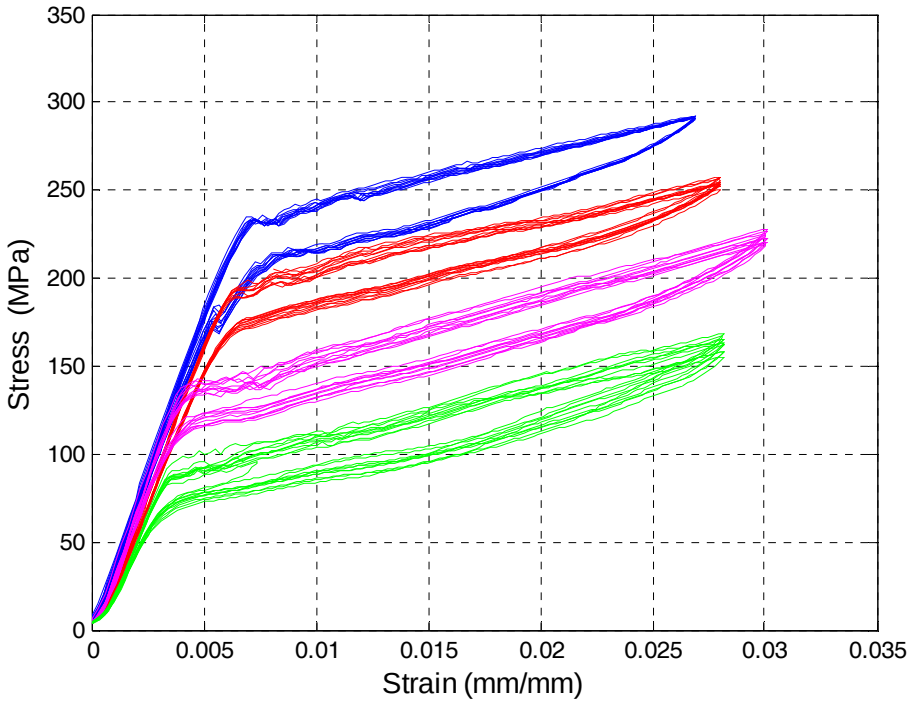

(a) batch 1, $\dot{\varepsilon} = 0.0012\ s^{-1}$

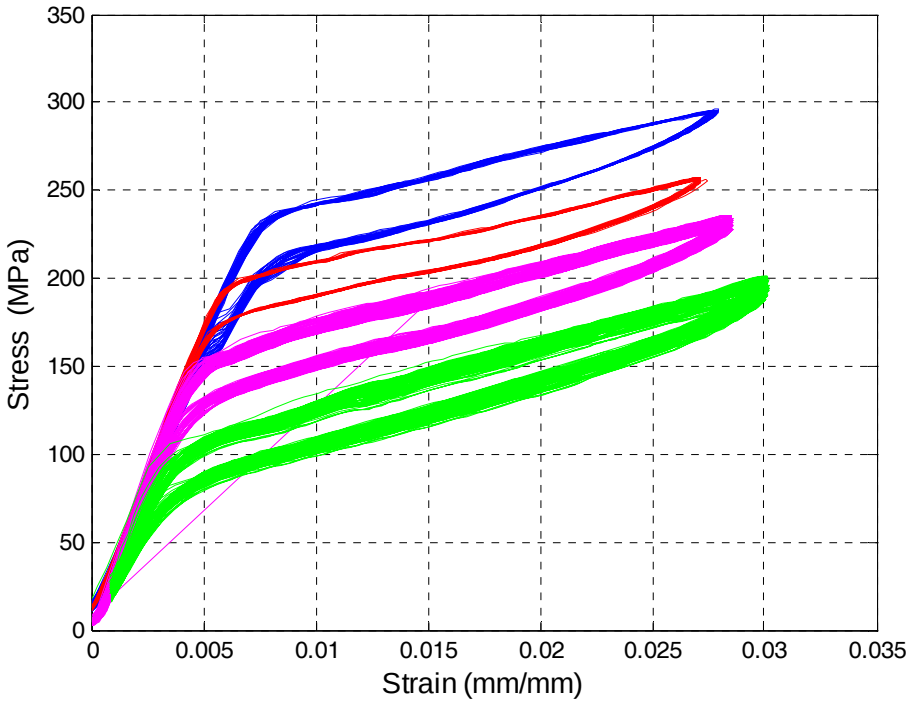

(b) batch 1 , $\dot{\varepsilon} = 0.06\ s^{-1}$

Figure 5. Stress-strain curves of Cu-Al-Be wires at various temperatures in batch 1: (a) loading frequency = 0.02 Hz; (b) loading frequency = 1 Hz

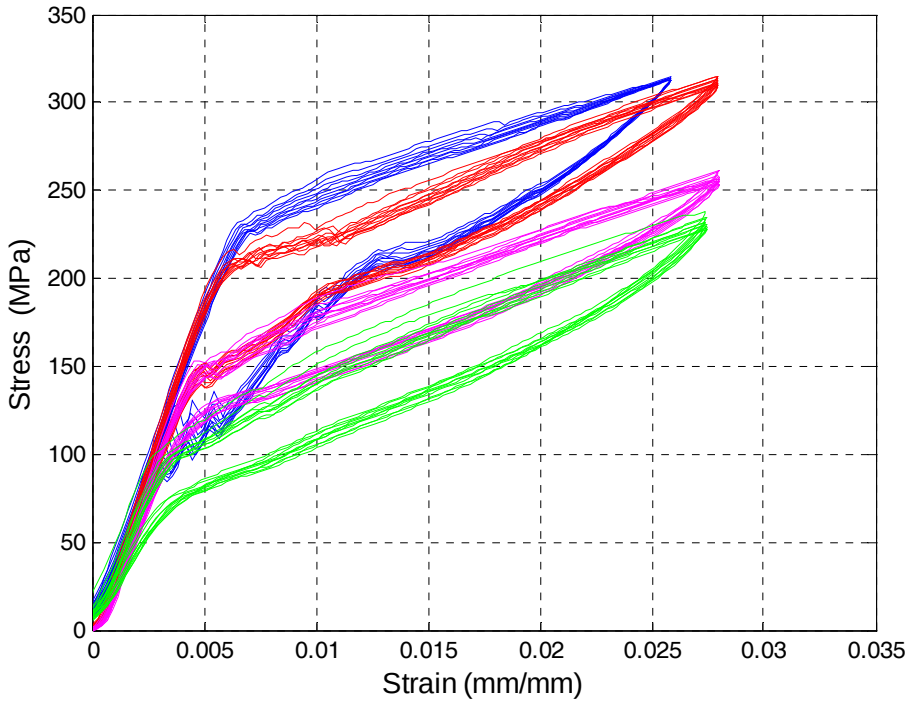

(a) batch 2, $\dot{\varepsilon} = 0.0012\ s^{-1}$

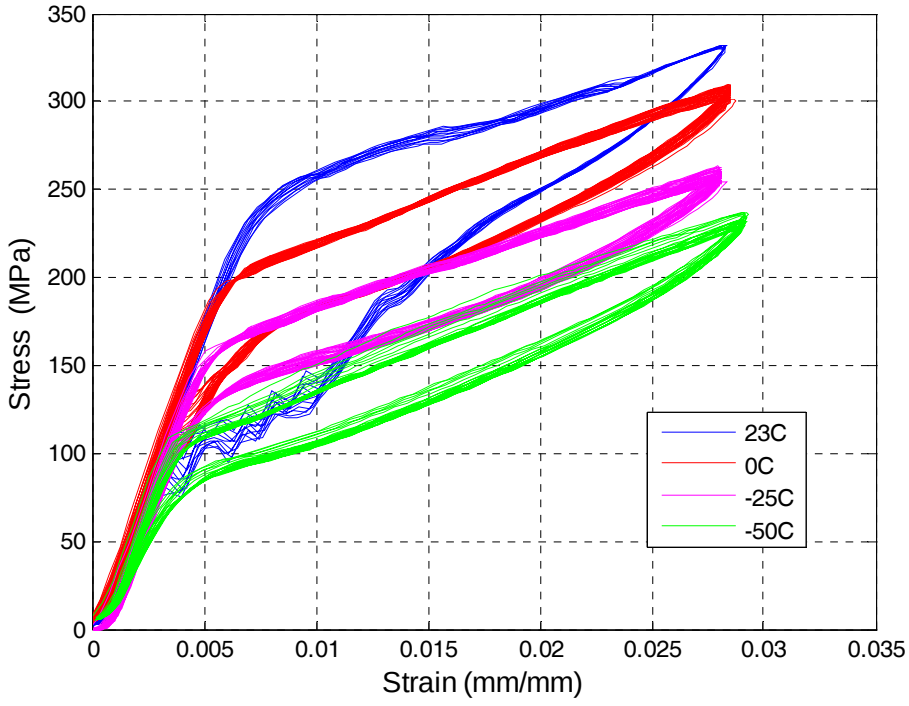

(b) batch 2, $\dot{\varepsilon} = 0.06\ s^{-1}$

Figure 6. Stress-strain curves of Cu-Al-Be wires at various temperatures in batch 2: (a) loading frequency = 0.02 Hz; (b) loading frequency = 1 Hz;

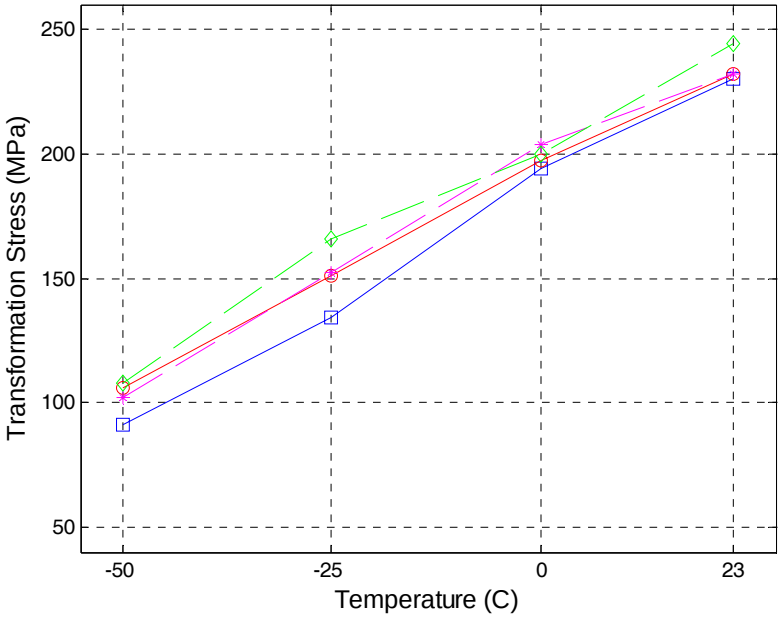

Figure 7. Variation of transformation stress of Cu-Al-Be wires with temperature (-□-: batch 1 & 0.0012 s^{-1}; -o-: batch 1 & 0.06 s^{-1}; - -*- -: batch 2 & 0.0012 s^{-1}; - -◊- -: batch 1 & 0.06 s^{-1})

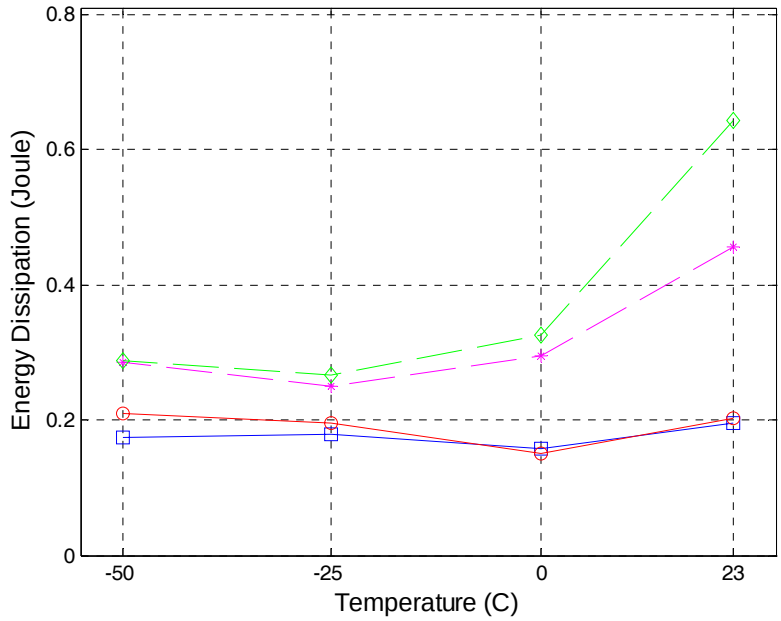

Figure 8. Variation of energy dissipation (per load cycle, normalized by maximum strain) of Cu-Al-Be wires with temperatures (-□-: batch 1 & 0.0012 s^{-1}; -o-: batch 1 & 0.06 s^{-1}; - -*- -: batch 2 & 0.0012 s^{-1}; - -◊- -: batch 1 & 0.06 s^{-1})

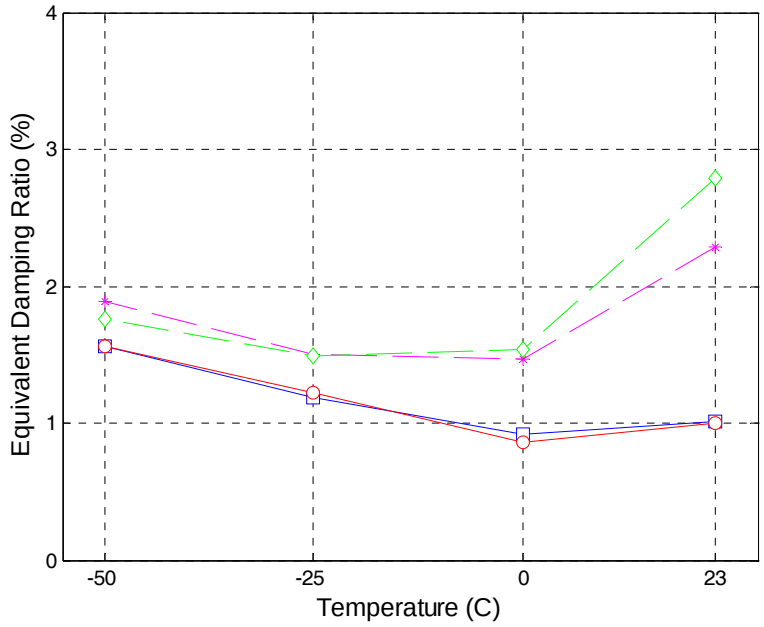

Figure 9. Variation of equivalent viscous damping ratio of Cu-Al-Be wires with temperatures (-□-: batch 1 & 0.0012 s^{-1}; -o-: batch 1 & 0.06 s^{-1}; - -*- -: batch 2 & 0.0012 s^{-1}; - -◊- -: batch 1 & 0.06 s^{-1})

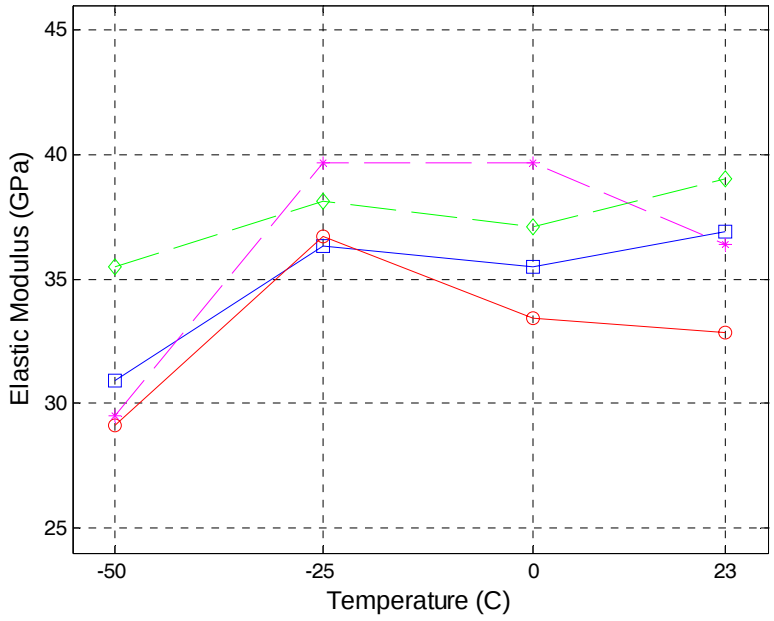

Figure 10. Variation of elastic modulus of Cu-Al-Be wires with temperature (-□-: batch 1 & 0.0012 s^{-1}; -o-: batch 1 & 0.06 s^{-1}; - -*- -: batch 2 & 0.0012 s^{-1}; - -◊- -: batch 1 & 0.06 s^{-1})

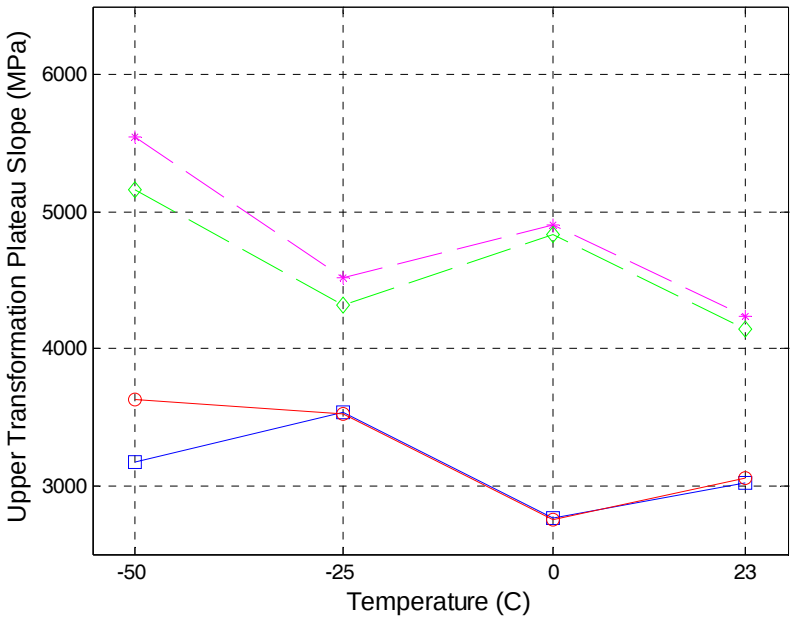

Figure 11. Variation of upper transformation plateau plateau of Cu-Al-Be wires with temperature (-□-: batch 1 & 0.0012 s^{-1}; -o-: batch 1 & 0.06 s^{-1}; - -*- -: batch 2 & 0.0012 s^{-1}; - -◊- -: batch 1 & 0.06 s^{-1})

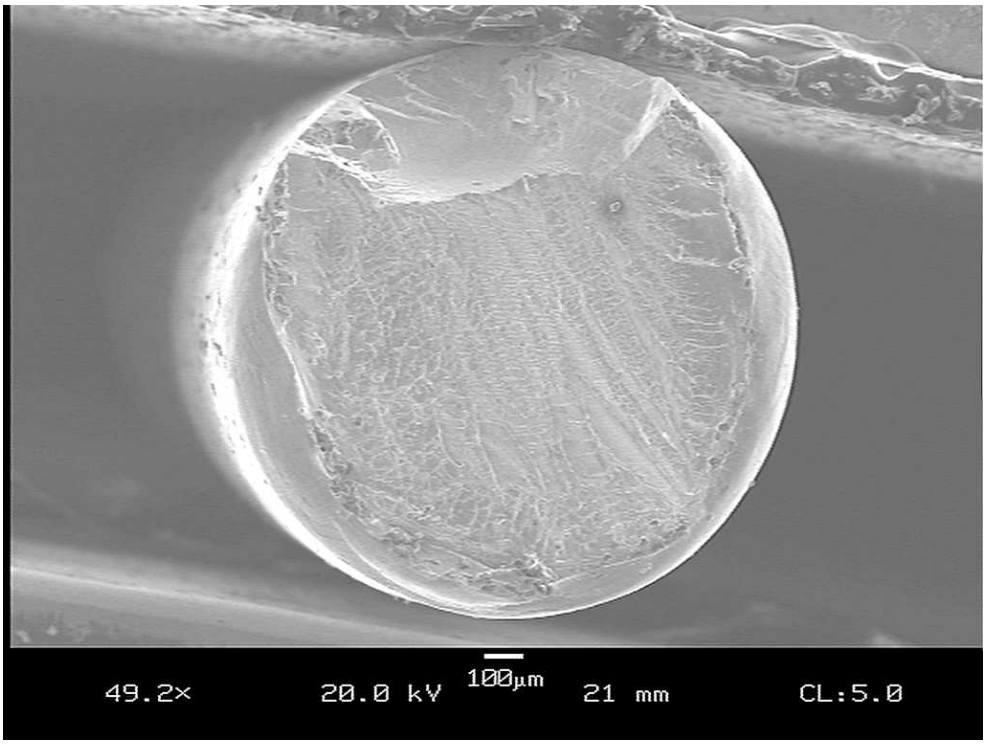

Figure 12. SEM picture of fracture surface of Cu-Al-Be wire failed under cyclic loading (1 Hz) at 0°C

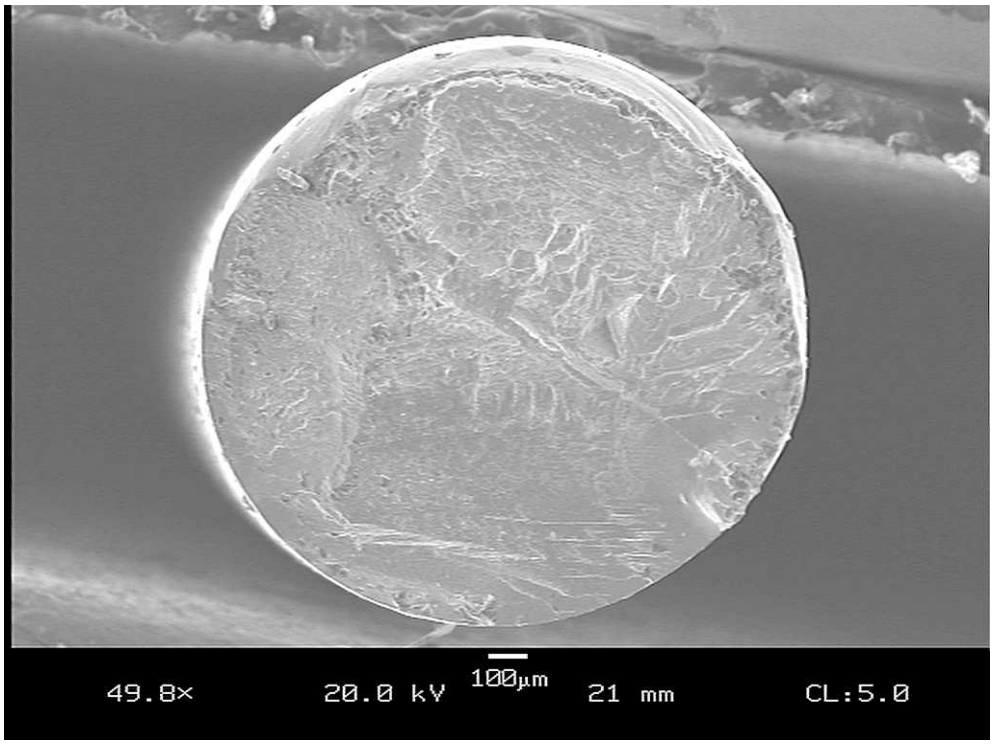

Figure 13. SEM picture of fracture surface of Cu-Al-Be wire failed under cyclic loading (1 Hz) at -25°C

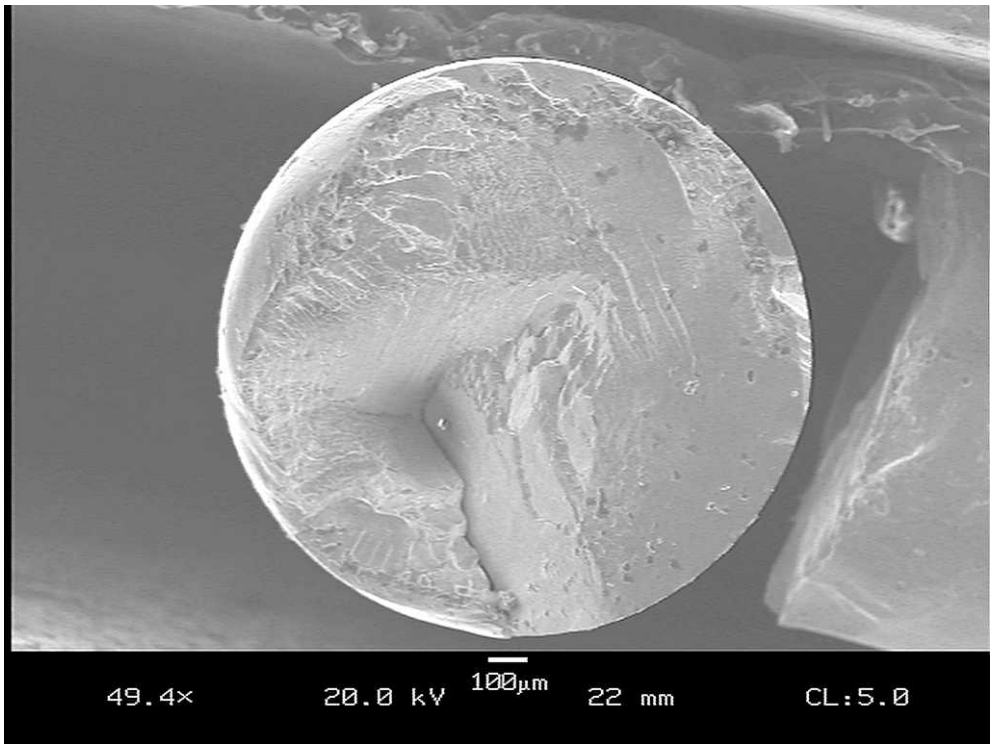

Figure 14. SEM picture of fracture surface of Cu-Al-Be wire failed under cyclic loading (1 Hz) at -50°C

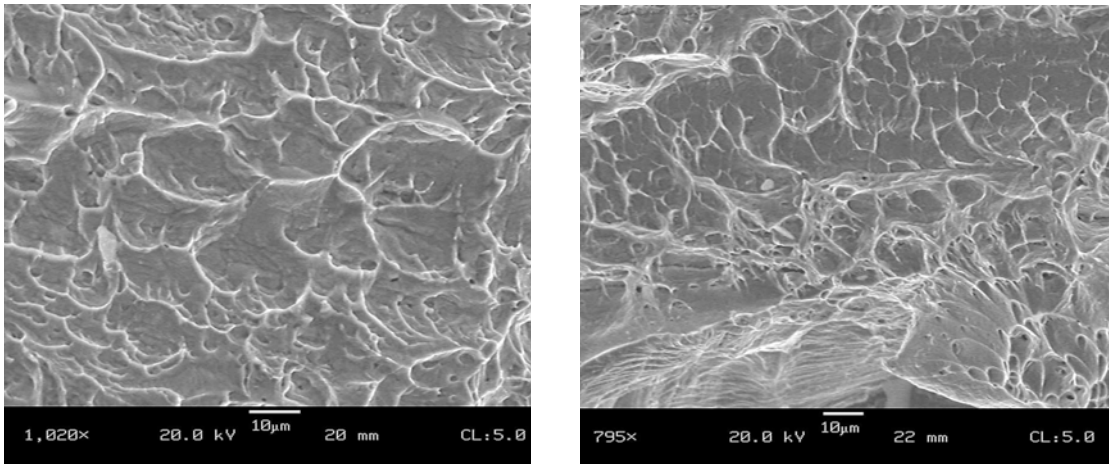

(a) (b)

Figure 15. SEM picture of local fracture surface of Cu-Al-Be wire failed under cyclic loading (1 Hz): (a) -25°C; (b) -50°C

Figure 16 shows the fatigue life of the Cu-Al-Be wires tested at various temperatures and loading rates under strain-controlled cyclic test. Observing the variation of fatigue life (expressed in terms of number of load cycles to failure) with respect to temperature, one can see that fatigue life generally decreases with increasing test temperature, apparently due to the increase in transformation stress.

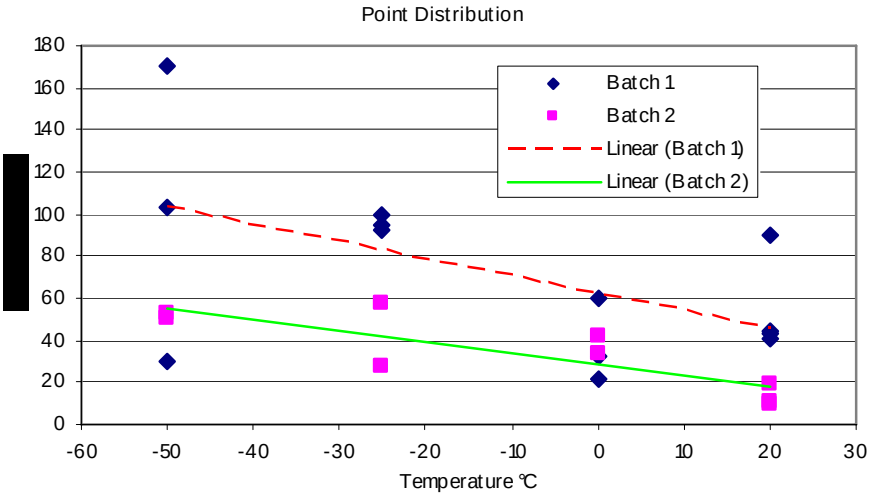

Figure 16. Number of load cycles to failure of Cu-Al-Be wires loaded at various temperatures (loading rate = 0.06 s^{-1})

The average number of cycles required to fracture a Cu-Al-Be specimen under 1 Hz loading frequency was calculated and is shown in Table 3. Comparing these numbers to different batches strongly suggests that different heat treatment may lead to a significant change in cyclical life of Cu-Al-Be wires. It is seen that batch 1 wires have much higher cyclic life than batch 2 wires. Beginning at 23ºC the average cyclical life for batch 1 wires is 54.8, compared to merely 13.3 for batch 2 wires. will fracture in 37 cycles, this number increases to where a -50ºC average sample will fracture in 81.2 cycles. At 0°C, although the average number of load cycles to fracture for batch 1 and batch 2 wires are very close (38.3 vs. 38), quite significant difference (60 vs. 42) can be observed in the peak number of load cycles to fracture. Therefore, the reason for close average values may be due to a batch 1 wire sample with defect. At -25°C and -50°C, the cyclic life of batch 1 wires is more than twice that of batch 2 wires, even considering the fact that the batch 1 and batch 2 wires have similar transformation stress values.

Table 3. Number of load cycles to failure of Cu-Al-Be wires loaded at various temperatures (strain rate = 0.06 s^{-1})

Temperature (ºC)	**# of Cycles to Fracture (Mean value)**		**# of Cycles to Fracture (Highest value)**	
	Batch 1	**Batch 2**	**Batch 1**	**Batch 2**
23	54.8	13.3	90	19
0	38.3	38.0	60	42
-25	96.0	43.0	100	58
-50	101.0	51.5	170	53

Monotonic tensile tests of Cu-Al-Be wires were done at temperatures of 20°C, 0°C, -25°C, and -50°C respectively. Monotonic testing was done at a slow loading rate (average strain rate on the order of $2x10^{-4}$ sec^{-1}). The wires for monotonic test are all

from batch 1. The results are shown in Figure 17 below. The transformation stress follows the same trend as that of the cyclic loading test, that is, with increasing temperature, the transformation stress increases. The fracture point of Cu-Al-Be under monotonic loading seems to have no correlation with test temperature in any way. The stress-strain curve of Cu-Al-Be wires does not exhibit the hardening behavior as superelastic Nitinol wire usually exhibit whenever large strain is reached. It is also seen that the slope of the upper transformation plateau of Cu-Al-Be wires tested at -50°C is larger than wires tested at other temperatures. This is consistent with the observations made earlier for cyclic loading test.

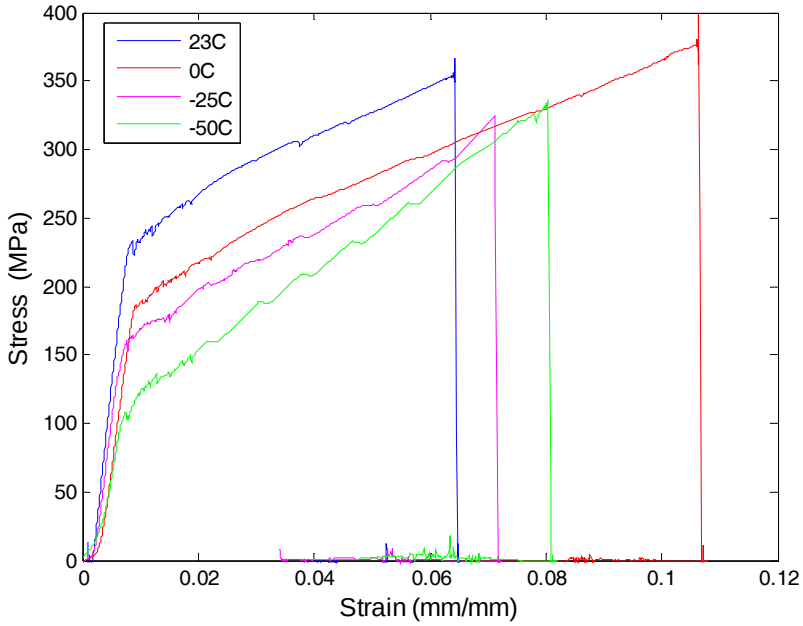

Figure 17. Stress-strain curves of Cu-Al-Be wires under monotonic load test

Figure 18 shows the stress-strain curves of Cu-Al-Be wires tested at extremely cold temperatures (loading rate = 0.06 s^{-1}) at -85ºC and -100ºC respectively. It is seen that the superelastic behavior of Cu-Al-Be wires is completely lost at -100ºC. In the unloading

process the strain is not fully recovered. At this point the wire is slack after unloading because it has been stretched out but cannot regain its original shape because its superelastic property is lost. Tests were also conducted to establish the austenite finish temperature A_f for the Cu-Al-Be wires in this study. Through a trial and error process it was determined that the minimum working temperature to maintain superelastic behavior is -85ºC for the Cu-Al-Be wires used in this study.

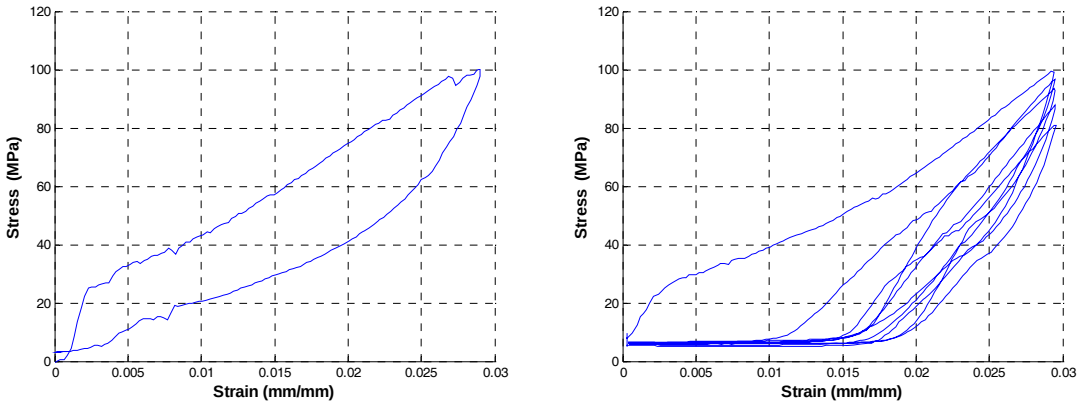

Figure 18. Stress-strain curves of superelastic Cu-Al-Be wires at extremely cold temperatures (loading rate = 0.06 s^{-1}): (a) -85ºC, (b) -100ºC (superelasticity is lost)

A comparative study of nickel titanium was necessary in order to evaluate the differences between NiTi and Cu-Al-Be. As seen in Figure 1, NiTi exhibits the same characteristic of having lower stress levels at lower temperatures. Figure 1 also shows that at 0°C NiTi is beginning to loose its superelastic ability while at -25°C NiTi completely lost its superelastic behavior. A comparison of the stress-strain relationships of NiTi and Cu-Al-Be wires at room temperature of 23°C is shown in Figure 19. NiTi's post yield characteristics show the stress to be steady for a short period and then attain high stress levels. Cu-Al-Be will have a maximum stress at least 200MPa less than that of

NiTi at 6% strain. Cu-Al-Be wires will also have a plateau stress level about 50MPa less on average than NiTi. Additionally, NiTi has been extensively researched by the writers and has been observed to last over 2000 load cycles at 8% strain. However, the longest lasting Cu-Al-Be wire tested in this study lasted only a mere 170 cycles at 3% strain. NiTi thus proves to have a superior fatigue life to Cu-Al-Be.

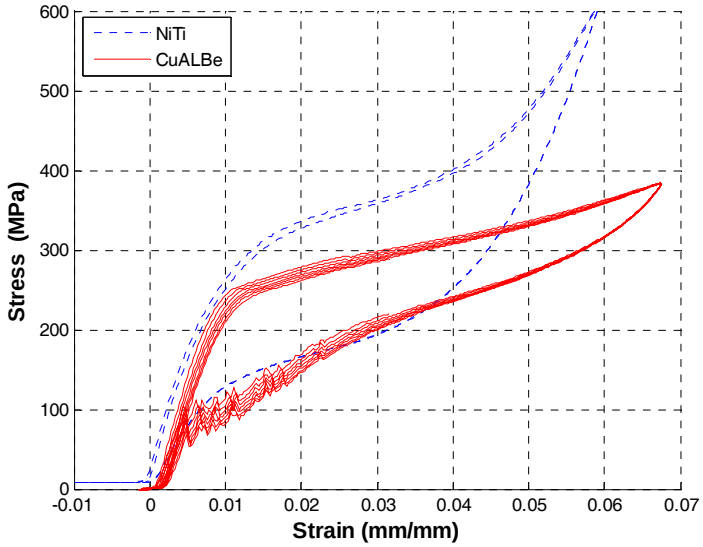

Figure 19. Stress-strain curves of Nitinol and Cu-Al-Be wires at 23°C (loading rate = 0.06 s^{-1})

Table 4. Details of Cu-Al-Be wires under cyclic testing at various temperatures

Mono. = monotonic loading test carried out to failure

Wires with the same number are the same wire with a different condition
Each wire is trained @ 1 Hz (3% Strain) for 5 cycles (a cycles); training data is denoted by symbol "a" while "b" refers to formal testing at designated temperature.

All dynamic tests were performed at 3% cyclic strain amplitude
* denotes heat treatment batch 2 of wires made on 7/11/2007 (20min@750c), otherwise batch 1 is used (30min@750c)

Test Date	Wire	Temperature (°C)	Frequency (Hz)	Cycles	Yield Point (MPa)	Post-Yield Stiffness Ratio
7/12/2007	1a	23	1	5		
7/12/2007	1b	23	0.02	10 NF	228	0.093
7/12/2007	2a	23	1	5		
7/12/2007	2b	23	1	45	240	0.092
7/12/2007	3a	23	1	5		
7/12/2007	3b	23	1	90	238	0.094
7/12/2007	4a	23	1	5		
7/12/2007	4b	23	1	43		
7/12/2007	5a	23	1	5		
7/12/2007	5b*	23	1	19	244	0.106
7/12/2007	6a	23	1	5		
7/12/2007	6b*	23	1	11	255	0.090
7/12/2007	7a	23	1	5		
7/12/2007	7b*	23	1	10		
7/12/2007	8a	23	1	5		
7/12/2007	8b	23	1	41	232	0.093
7/12/2007	9a	23	1	5		
7/12/2007	9b	23	0.02	10 NF	238	0.103
7/12/2007	10a	23	1	5		
7/12/2007	10b	23	0.02	10 NF	230	0.082
7/12/2007	11a	23	1	5		
7/12/2007	11b*	23	0.02	10 NF	234	0.098
7/12/2007	12a	23	1	5		
7/12/2007	12b*	23	0.02	10 NF		
7/12/2007	13a	23	1	5		
7/12/2007	13b*	23	0.02	10 NF	232	0.117
Test Date	**Wire**	**Temperature (°C)**	**Frequency (Hz)**	**Cycles**	**Yield Point (MPa)**	**Post-Yield Stiffness Ratio**

7/13/2007	1a	23	1	5		
7/13/2007	1b	-50	1	30	109	0.109
7/13/2007	2a	23	1	5		
7/13/2007	2b	-50	1	103	106	0.125
7/13/2007	3a	23	1	5		
7/13/2007	3b	-50	1	170	98	0.109
7/13/2007	4a	23	1	5		
7/13/2007	4b*	-50	1	50	122	0.138
7/13/2007	5a	23	1	5		
7/13/2007	5b*	-50	1	53	108	0.145
Test Date	**Wire**	**Temperature (°C)**	**Frequency (Hz)**	**Cycles**	**Yield Point (MPa)**	**Post-Yield Stiffness Ratio**
7/16/2007	1a	23	1	5		
7/16/2007	1b	-50	0.02	10 NF	97	0.126
7/16/2007	1c	-100	0.02	5 NF		
7/16/2007	1d	23	0.02	5 NF		
7/16/2007	2a	23	1	5		
7/16/2007	2b	-50	0.02	10 NF	91	0.103
7/16/2007	3a	23	1	5		
7/16/2007	3b	-50	0.02	10 NF	90	0.131
7/16/2007	4a*	23	1	5		
7/16/2007	4b*	-50	0.02	10 NF	102	0.166
7/16/2007	5a*	23	1	5		
7/16/2007	5b*	-50	0.02	10 NF	102	0.188
7/16/2007	5c*	23►-200	1	150 NF		
Test Date	**Wire**	**Temperature (°C)**	**Frequency (Hz)**	**Cycles**	**Yield Point (MPa)**	**Post-Yield Stiffness Ratio**
7/18/2007	1a	23	1	5		
7/18/2007	1b	-25	1	100	156	0.103
7/18/2007	2a	23	1	5		
7/18/2007	2b	-25	1	95	151	0.096
7/18/2007	3a	23	1	5		
7/18/2007	3b	-25	1	93	155	0.090
7/18/2007	4a*	23	1	5		
7/18/2007	4b*	-25	1	58	166	0.113
7/18/2007	5a*	23	1	5		
7/18/2007	5b*	-25	1	28	162	0.138

7/18/2007	6a	23	1	5		
7/18/2007	6b	-25	0.02	10 NF	138	0.101
7/18/2007	7a	23	1	5		
7/18/2007	7b	-25	0.02	10 NF	134	0.097
7/18/2007	8a	23	1	5		
7/18/2007	8b	-25	0.02	10 NF	138	0.108
7/18/2007	9a*	23	1	5		
7/18/2007	9b*	-25	0.02	10 NF	152	0.114
7/18/2007	10a*	23	1	5		
7/18/2007	10b*	-25	0.02	10 NF	140	0.156
7/18/2007	11a	23	1	5		
7/18/2007	11b	0	1	22	197	0.082
7/18/2007	12a	23	1	5		
7/18/2007	12b	0	1	60	196	0.098
7/18/2007	13a	23	1	5		
7/18/2007	13b	0	1	33	194	0.075
7/18/2007	14a*	23	1	5		
7/18/2007	14b*	0	1	42	200	0.130
7/18/2007	15a*	23	1	5		
7/18/2007	15b*	0	1	34	208	0.107
Test Date	**Wire**	**Temperature (°C)**	**Frequency (Hz)**	**Cycles**	**Yield Point (MPa)**	**Post-Yield Stiffness Ratio**
7/20/2007	1a	23	1	5		
7/20/2007	1b	0	0.02	10 NF	200	0.109
7/20/2007	2a	23	1	5		
7/20/2007	2b	0	0.02	10 NF	194	0.078
7/20/2007	3a	23	1	5		
7/20/2007	3b	0	0.02	10 NF	191	0.094
7/20/2007	4a*	23	1	5		
7/20/2007	4b*	0	0.02	10 NF	200	0.119
7/20/2007	5a*	23	1	5		
7/20/2007	5b*	0	0.02		204	0.124
7/20/2007	6a	23	1			
7/20/2007	6b	-75	0.02			
7/20/2007	6c	-85	0.02			
7/20/2007	6d	-85	0.02			
7/20/2007	7	23	0.02 Mono.			

7/20/2007	8	-50	0.02 Mono.			
7/20/2007	9	-25	0.02 Mono.			
7/20/2007	10	0	0.02 Mono.			
7/20/2007	11	0	0.02 Mono.			

Table 5. Averages of the plateau slope, elastic slope, post-yield stiffness ratio, and yield point.

The plateau slope is the value of the graphically measured slope of the best fit line of the curve occurring after the yield point on a stress versus strain graph.

The elastic slope is the value of the graphically measured slope of the best fit line of the curve occurring before the yield point on a stress versus strain graph.

The post stiffness yield ratio is calculated by dividing the plateau slope by the elastic slope

Frequency (Hz)	Batch	Temperature (°C)	Plateau Slope	Elastic Slope	Post-Yield Stiffness Ratio	Yield Point (MPa)
0.02	1	23	3106.81	33803.08	0.09	232.00
0.02	1	0	3323.71	35568.74	0.09	195.00
0.02	1	-25	3605.53	35260.52	0.10	136.17
0.02	1	-50	3597.70	30068.63	0.12	92.50
0.02	2	23	4040.66	37762.42	0.11	232.75
0.02	2	0	4741.30	39076.13	0.12	202.00
0.02	2	-25	4843.86	36418.94	0.13	146.00
0.02	2	-50	5100.12	28810.50	0.18	101.75
1	1	23	3270.85	35291.89	0.09	236.50
1	1	0	2925.15	34415.43	0.09	195.50
1	1	-25	3426.46	35553.82	0.10	153.67
1	1	-50	3560.90	31245.82	0.11	104.17
1	2	23	3847.49	39207.40	0.10	249.00
1	2	0	4302.03	36126.51	0.12	203.50
1	2	-25	4810.39	38283.54	0.13	163.50
1	2	-50	4644.34	32716.26	0.14	115.10

Frequency (Hz)			Plateau Slope	Elastic Slope	Post-Yield Stiffness Ratio	Yield Point (MPa)
0.02			4044.96	34596.12	0.12	167.27
1			3848.45	35355.08	0.11	177.62
	Batch					
	1		3352.14	33900.99	0.10	168.19
	2		4541.27	36050.21	0.13	176.70
		Temperature (°C)				
		23	3566.46	36516.20	0.098	237.56
		0	3823.05	36296.70	0.105	199.00
		-25	4171.56	36379.21	0.115	149.83
		-50	4225.76	30710.30	0.138	103.38

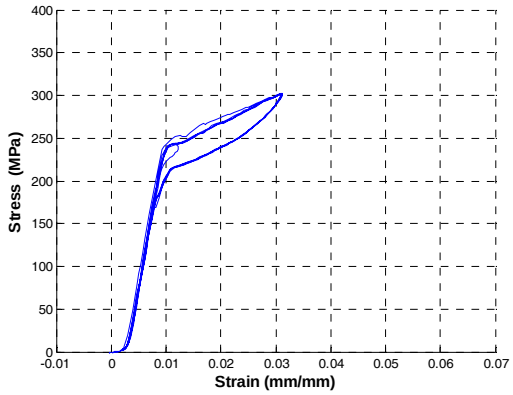

(a) Wire 1a

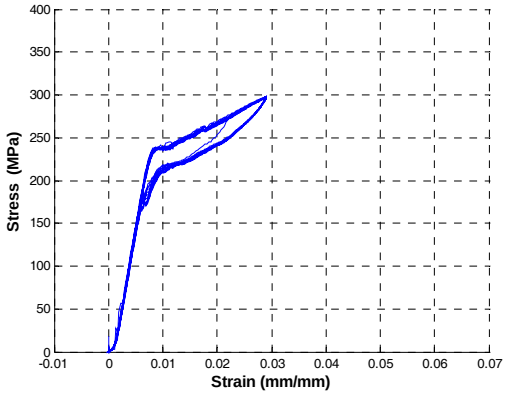

(b) Wire 1b

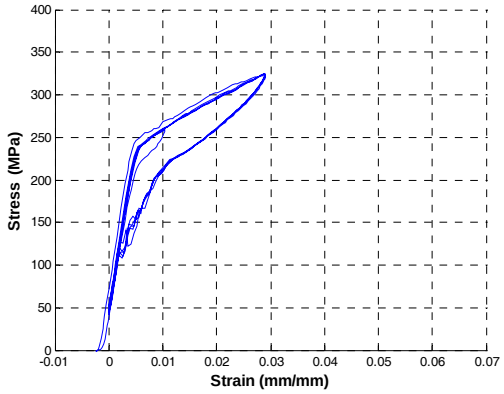

(c) Wire 2a

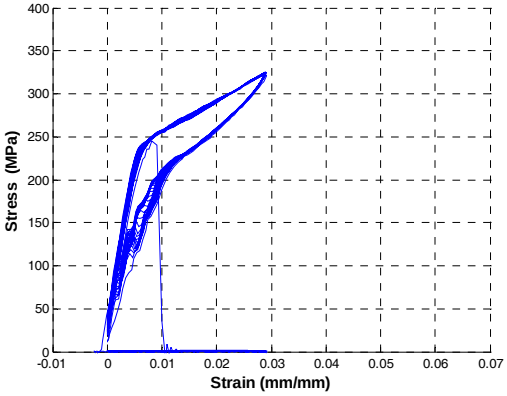

(d) Wire 2b

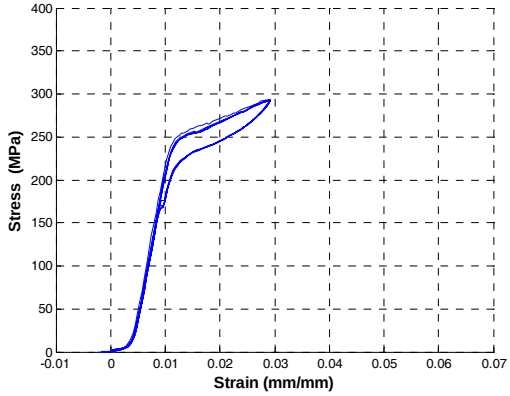

(e) Wire 3a

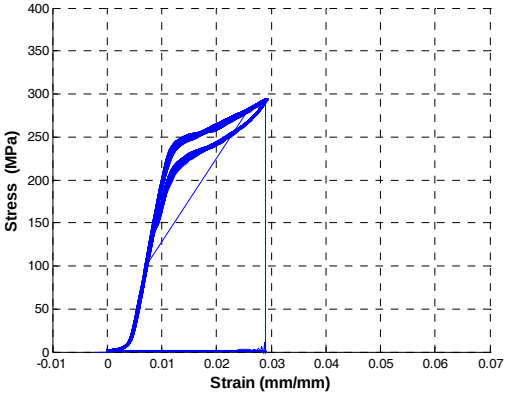

(f) Wire 3b

Figure 20. Results of Cu-Al-Be wires tested on 7/12/2007

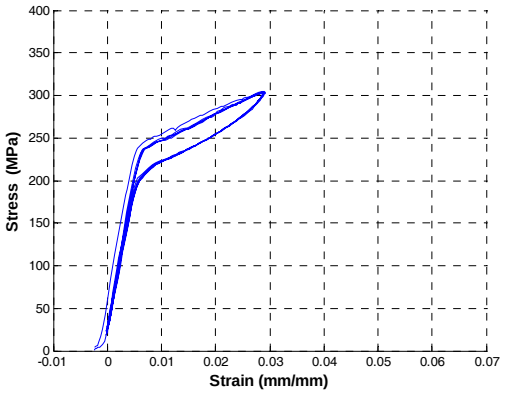

(a) Wire 4a

(b) Wire 4b (not available)

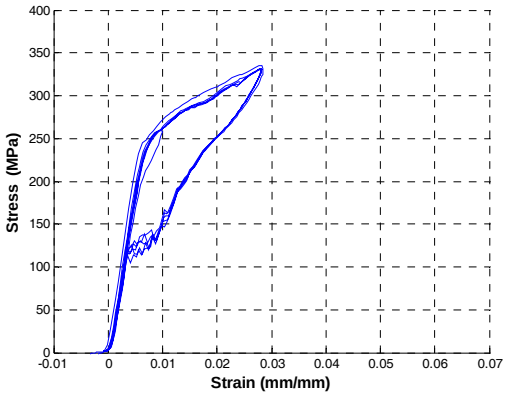

(c) Wire 5a

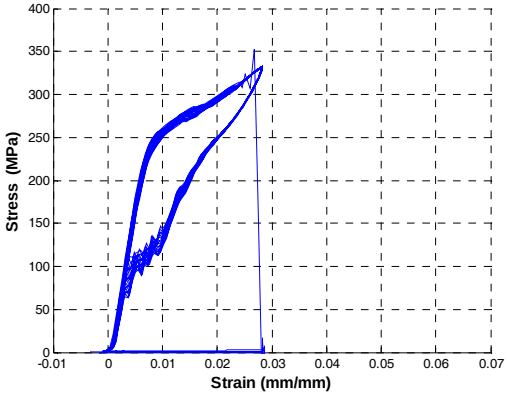

(d) Wire 5b

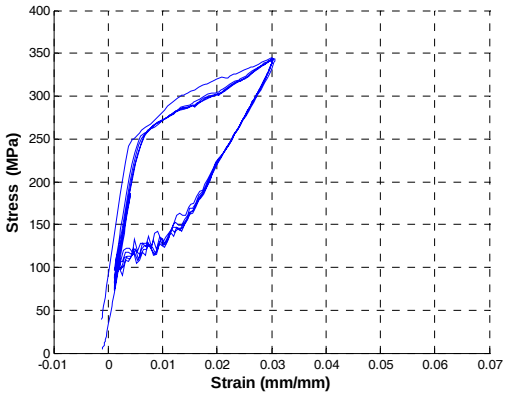

(e) Wire 6a

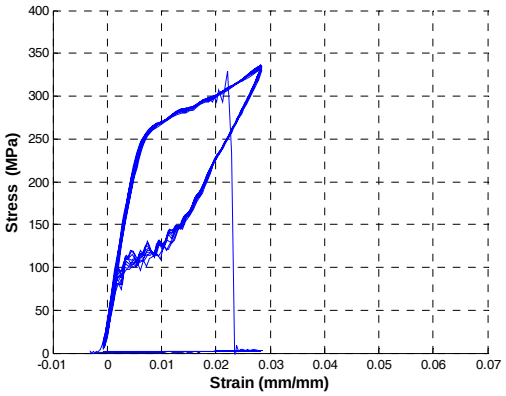

(f) Wire 6b

Figure 21. Results of Cu-Al-Be wires tested on 7/12/2007

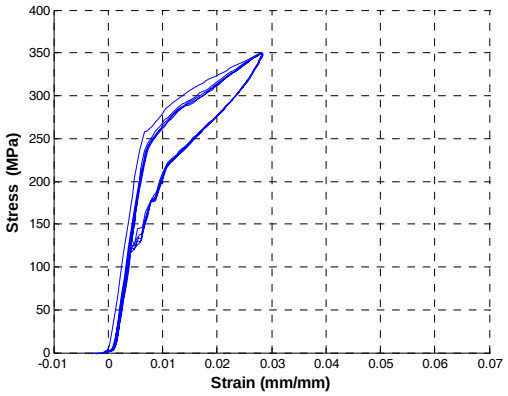

(a) Wire 7a

(b) Wire 7b (not available)

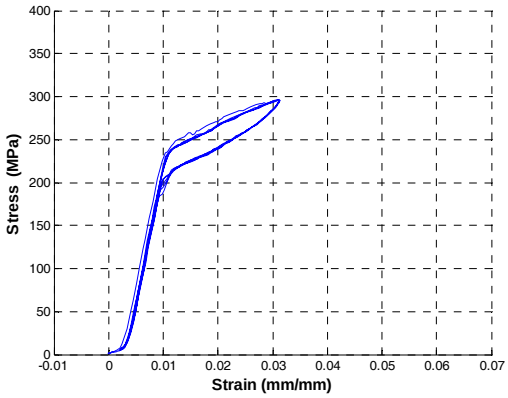

(c) Wire 8a

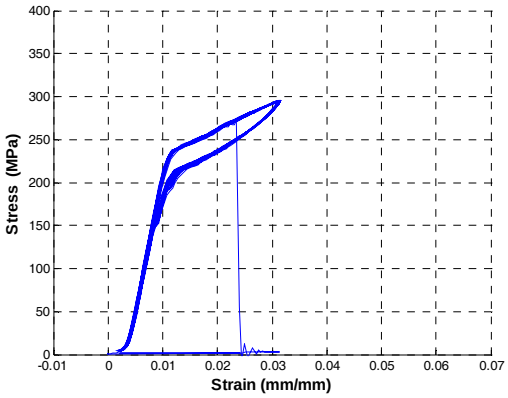

(d) Wire 8b

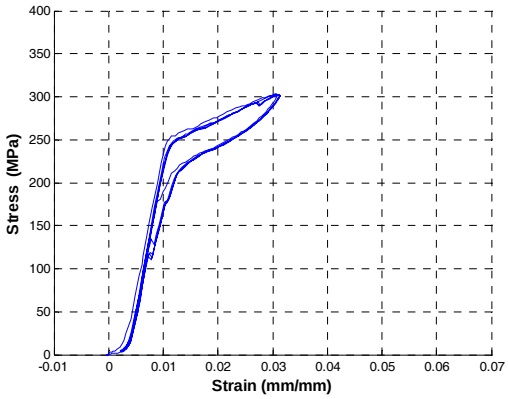

(e) Wire 9a

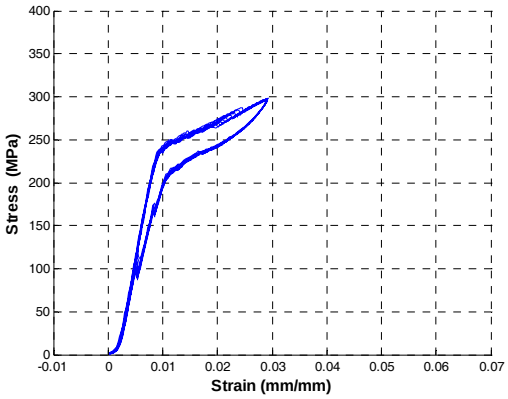

(f) Wire 9b

Figure 22. Results of Cu-Al-Be wires tested on 7/12/2007

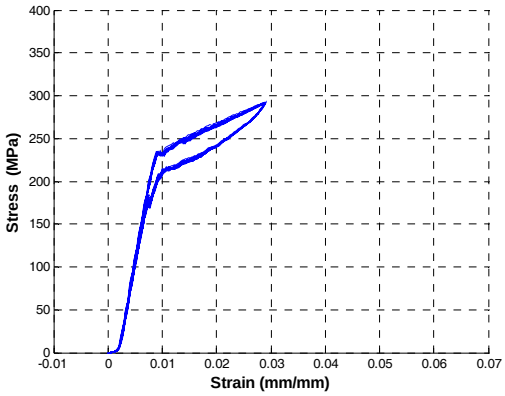

(a) Wire 10a (not available)

(b) Wire 10b

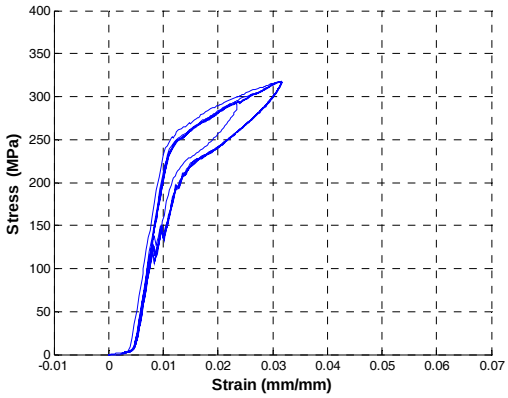

(c) Wire 11a

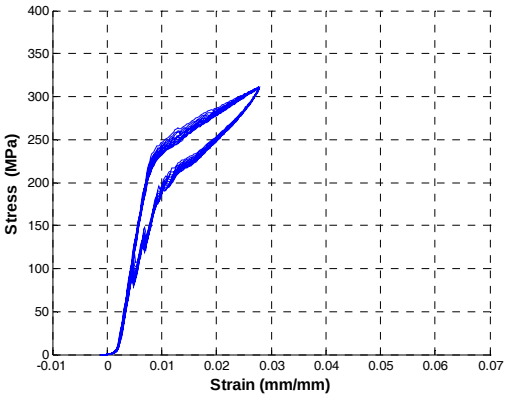

(d) Wire 11b

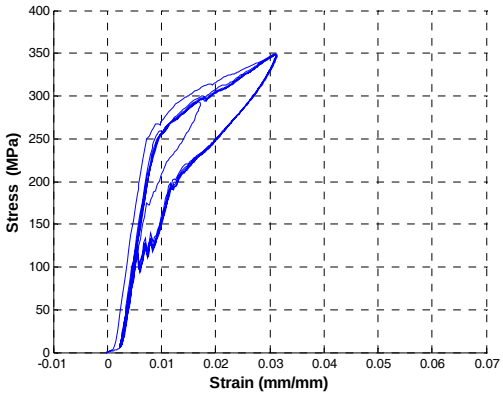

(e) Wire 12a

(f) Wire 12b (not available)

Figure 23. Results of Cu-Al-Be wires tested on 7/12/2007

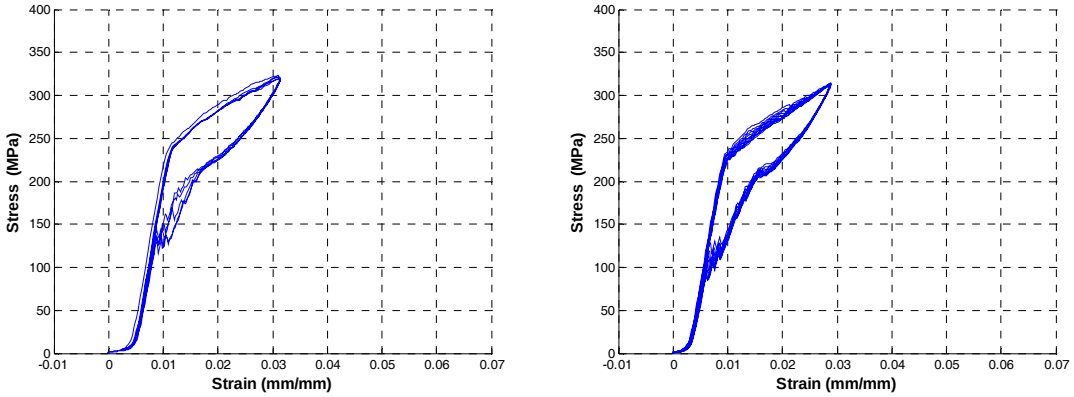

(a) Wire 13a (b) Wire 13b

Figure 24. Results of Cu-Al-Be wires tested on 7/12/2007

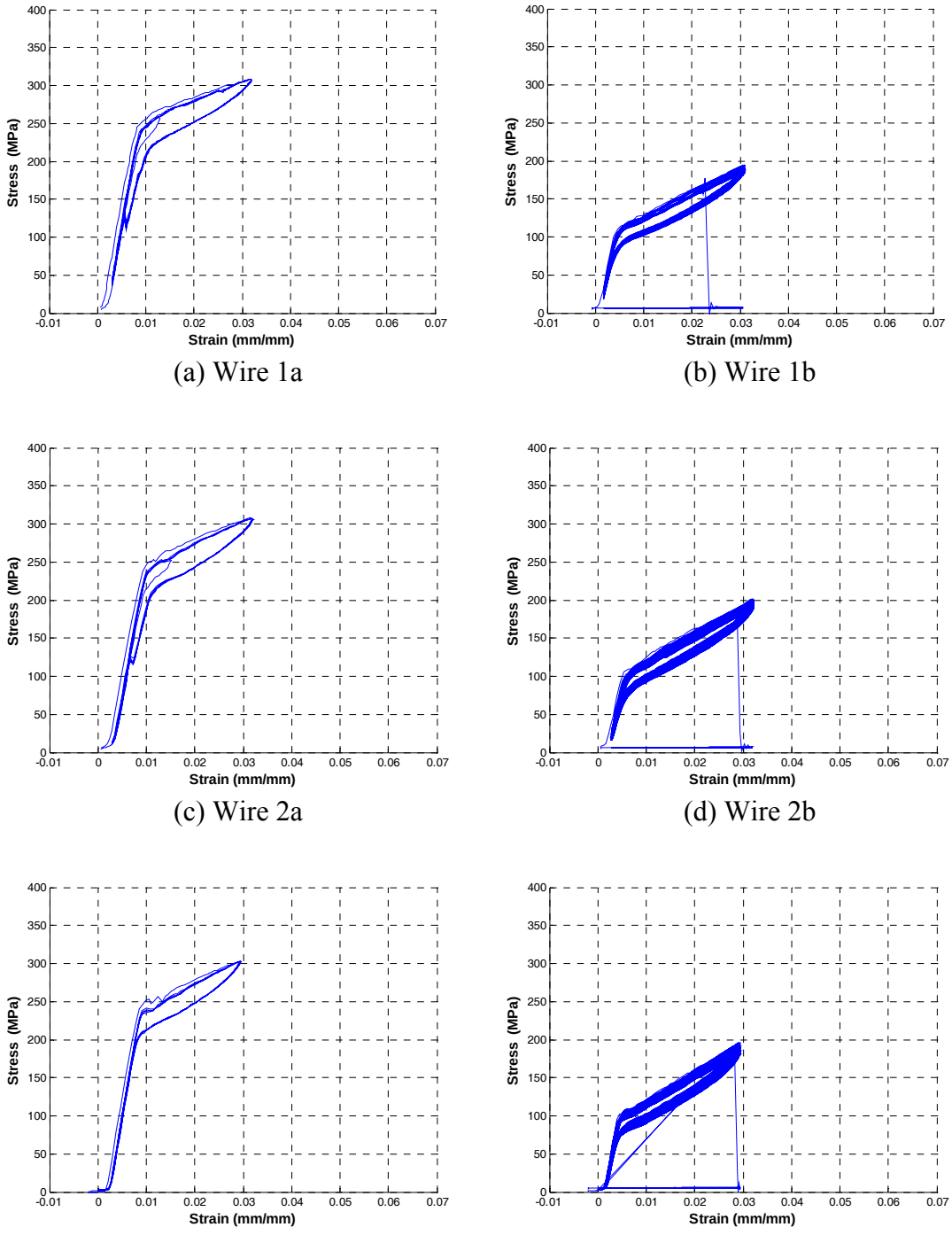

Figure 25. Results of Cu-Al-Be wires tested on 7/13/2007

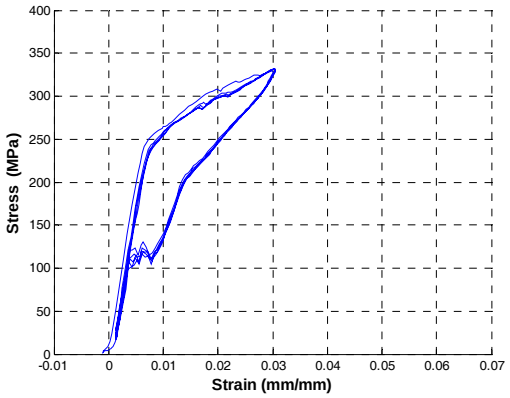

(a) Wire 4a

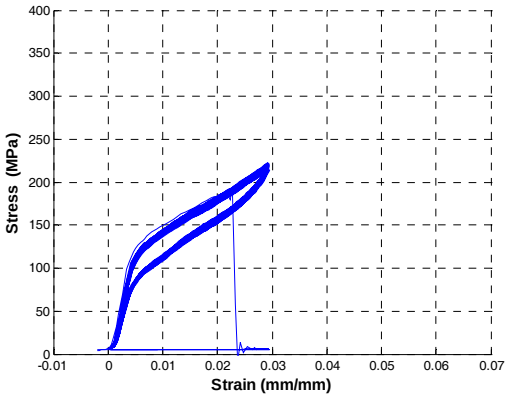

(b) Wire 4b

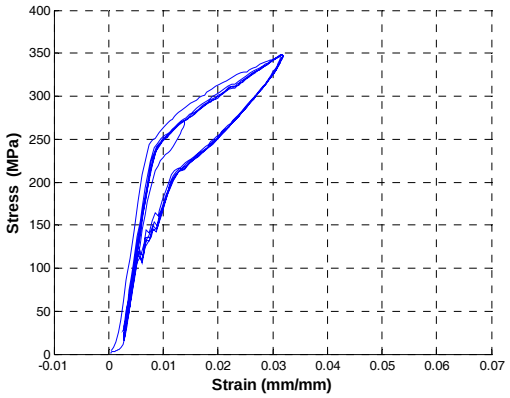

(a) Wire 5a

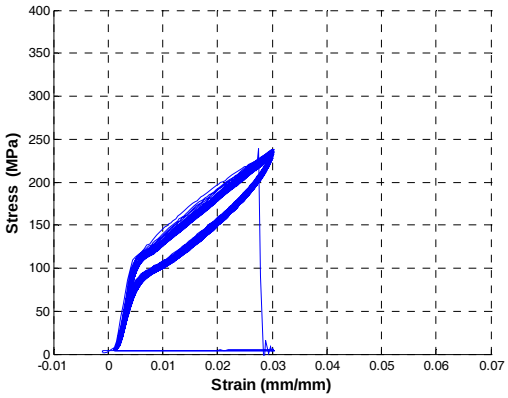

(b) Wire 5b

Figure 26. Results of Cu-Al-Be wires tested on 7/13/2007

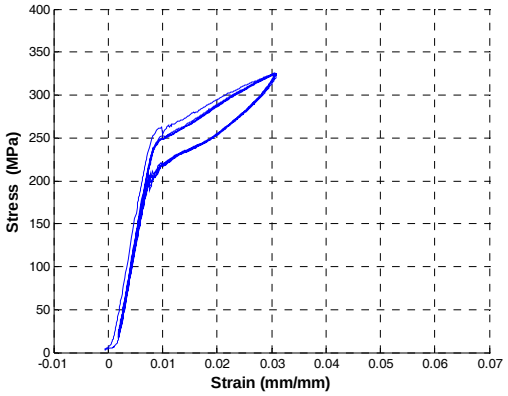

(a) Wire 1a

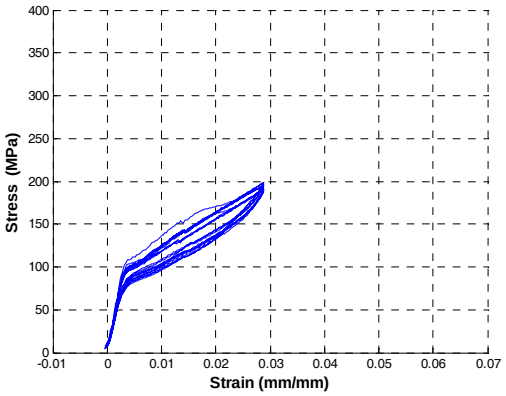

(b) Wire 1b

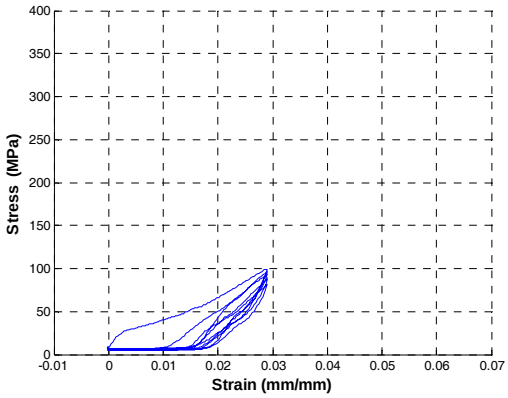

(c) Wire 1c

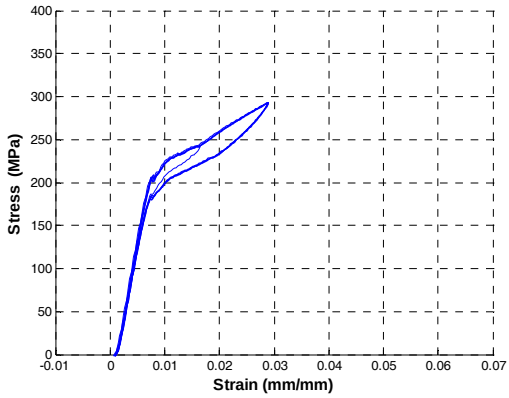

(d) Wire 1d

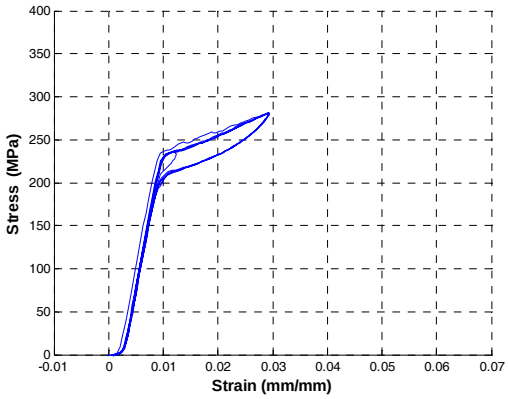

(e) Wire 2a

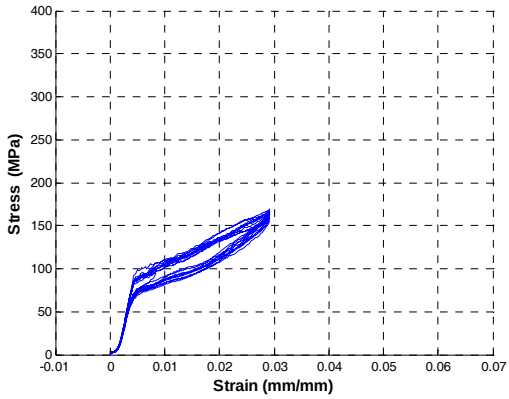

(f) Wire 2b

Figure 27. Results of Cu-Al-Be wires tested on 7/16/2007

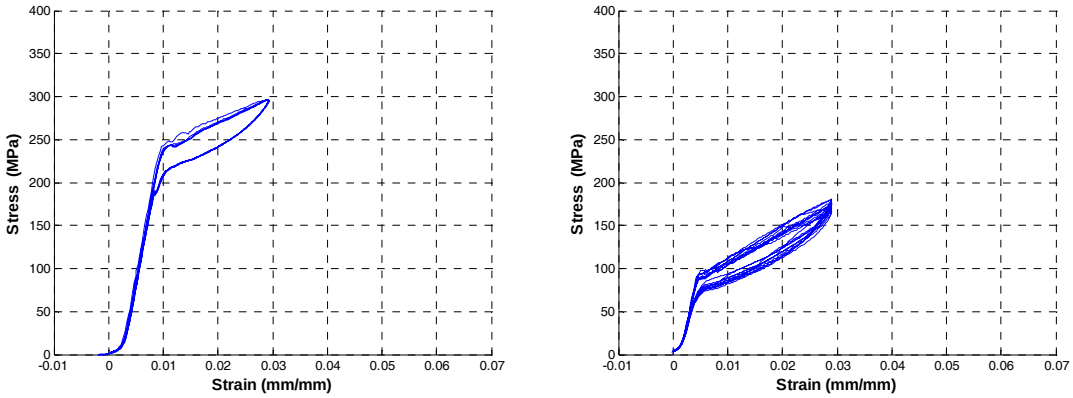

(a) Wire 3a

(b) Wire 3b

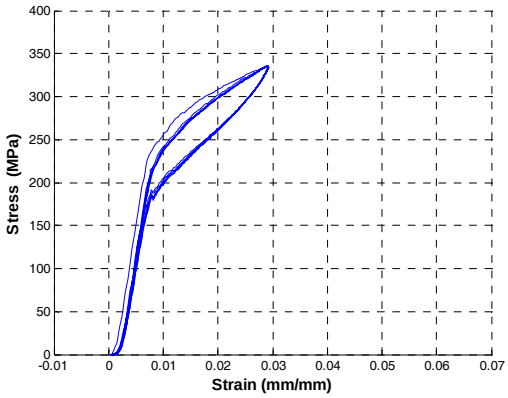

(c) Wire 4a

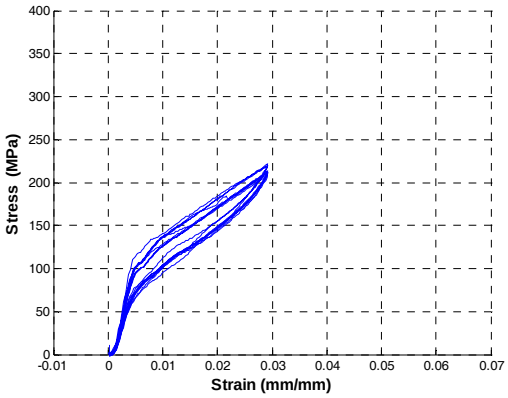

(d) Wire 4b

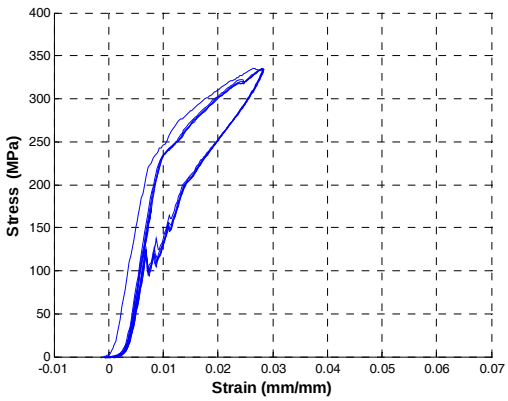

(e) Wire 5a

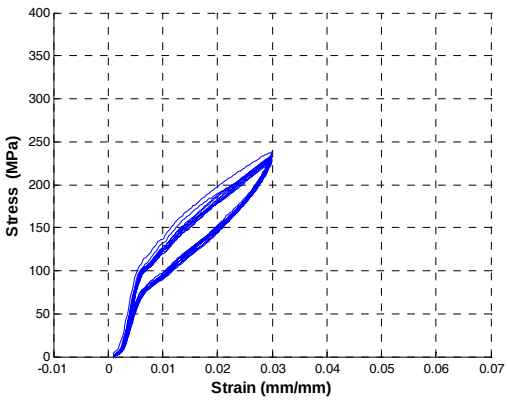

(f) Wire 5b

Figure 28. Results of Cu-Al-Be wires tested on 7/16/2007

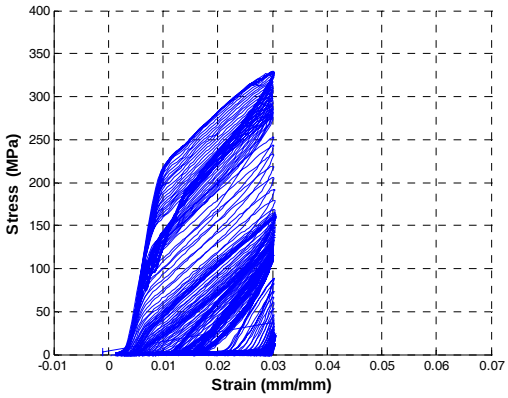

(a) Wire 5c

Figure 29. Results of Cu-Al-Be wires tested on 7/16/2007

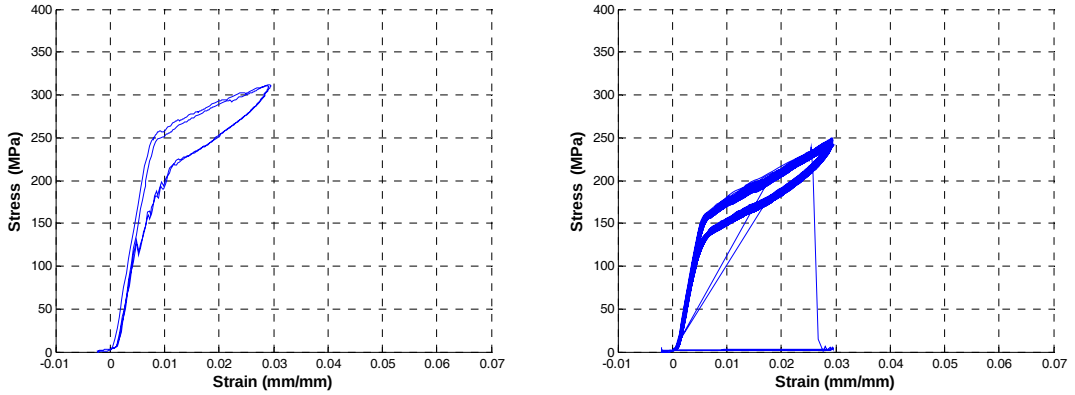

(a) Wire 1a (b) Wire 1b

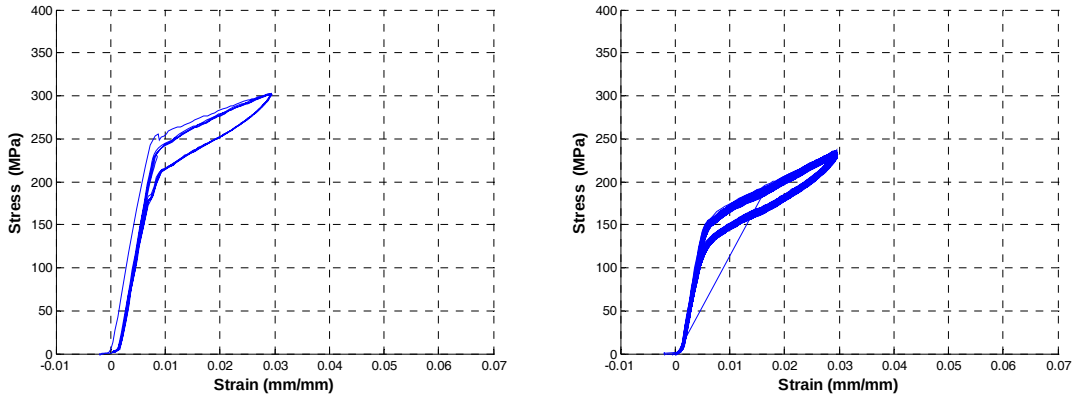

(c) Wire 2a (d) Wire 2b

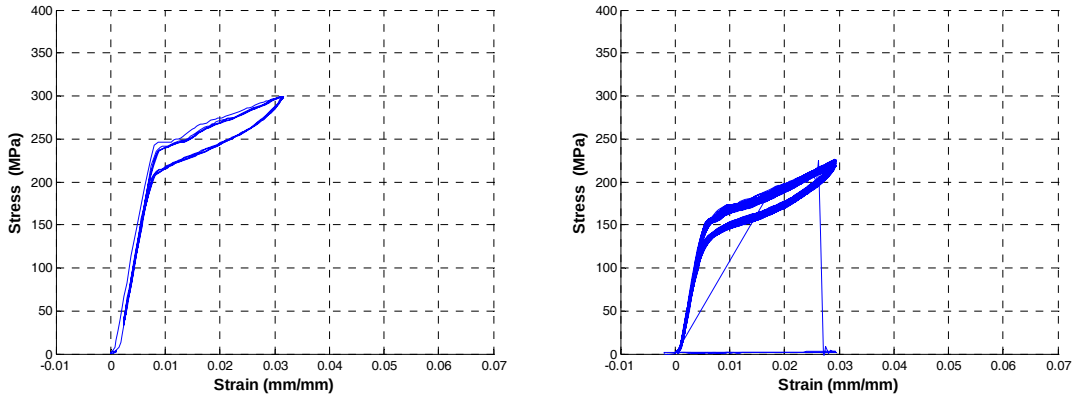

(e) Wire 3a (f) Wire 3b

Figure 30. Results of Cu-Al-Be wires tested on 7/18/2007

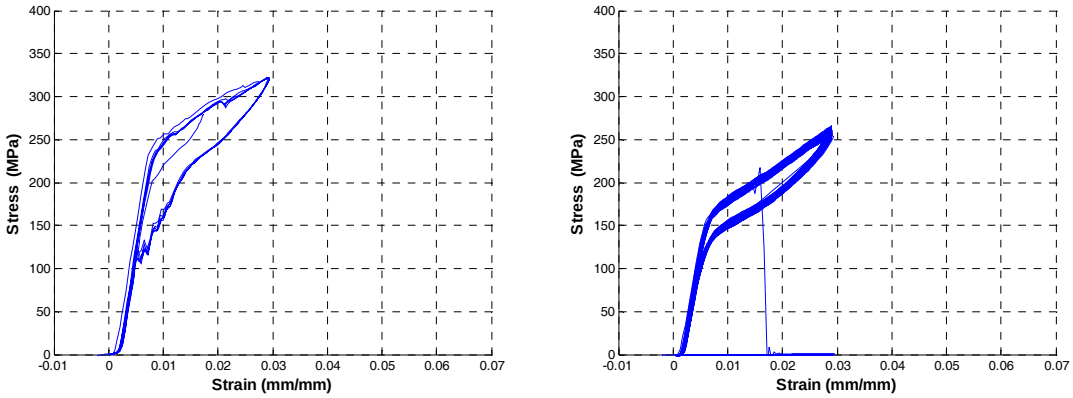

(a) Wire 4a

(b) Wire 4b

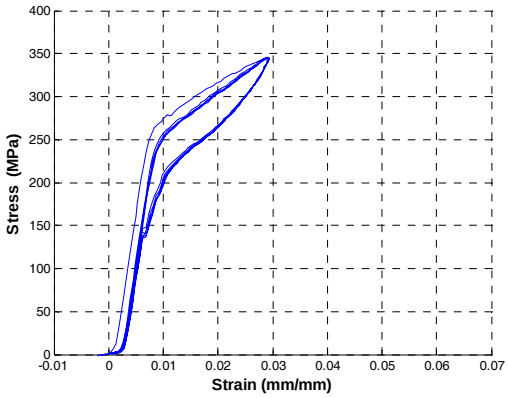

(c) Wire 5a

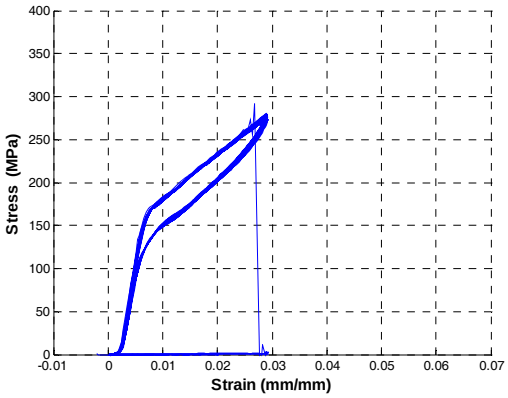

(d) Wire 5b

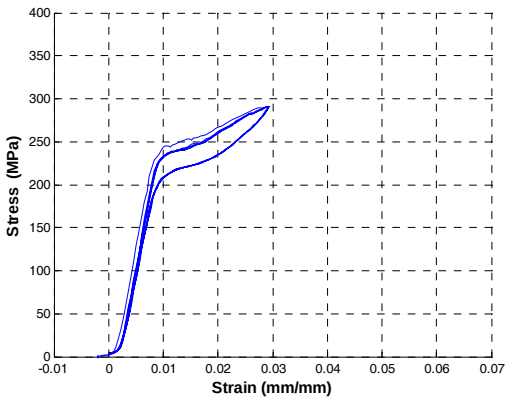

(e) Wire 6a

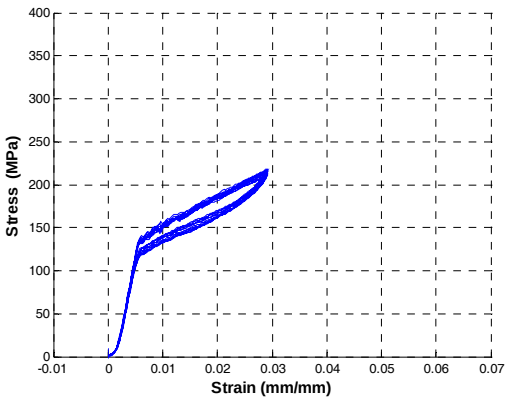

(f) Wire 6b

Figure 31. Results of Cu-Al-Be wires tested on 7/18/2007

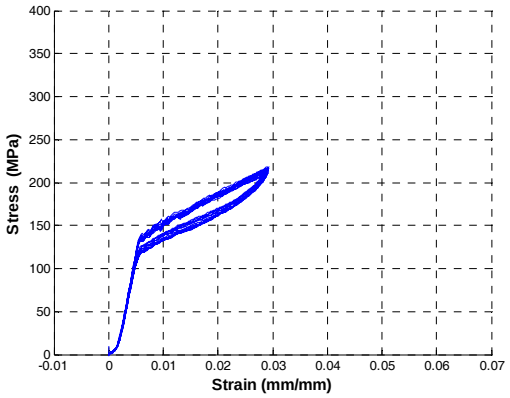

(a) Wire 7a

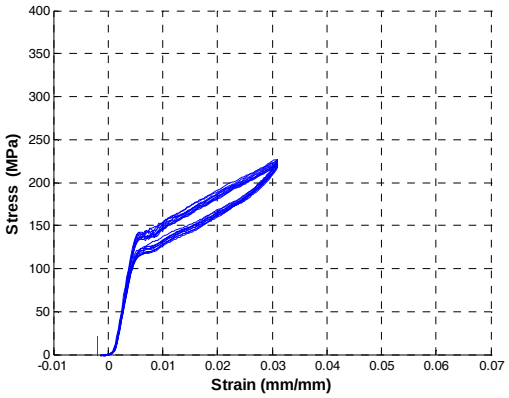

(b) Wire 7b

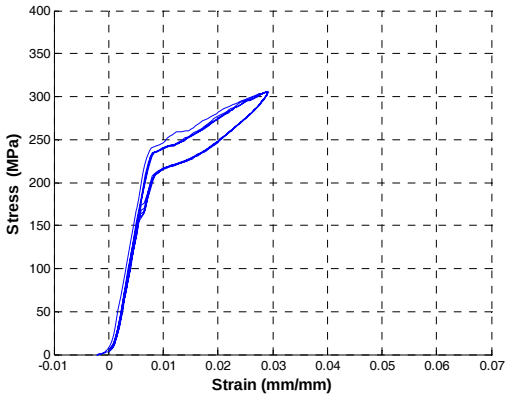

(c) Wire 8a

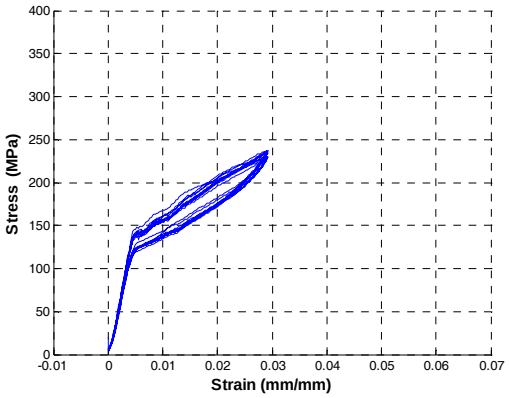

(d) Wire 8b

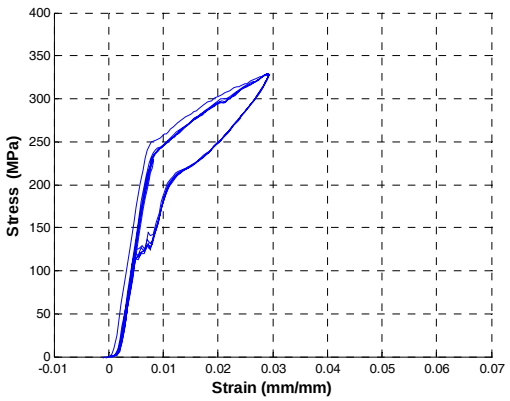

(e) Wire 9a

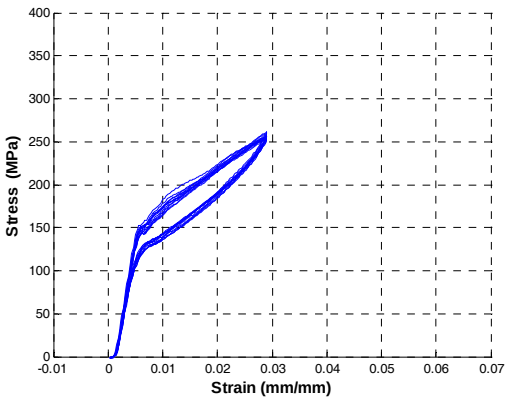

(f) Wire 9b

Figure 32. Results of Cu-Al-Be wires tested on 7/18/2007

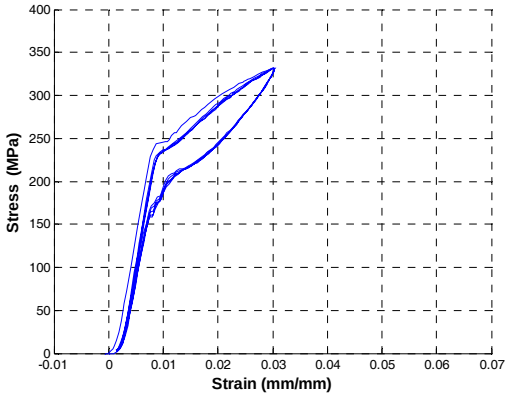

(a) Wire 10a

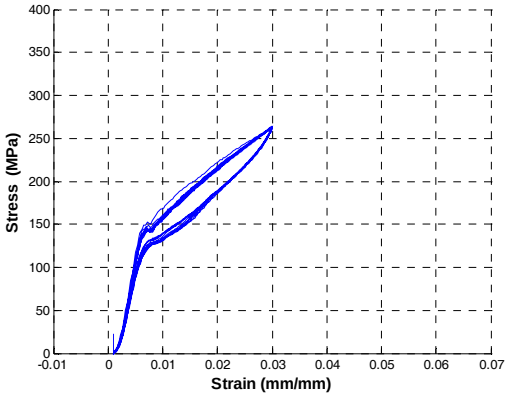

(b) Wire 10b

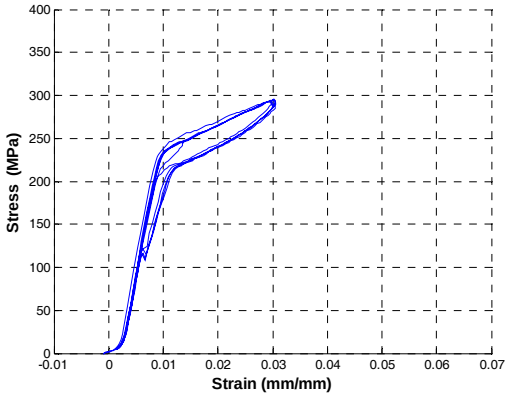

(c) Wire 11a

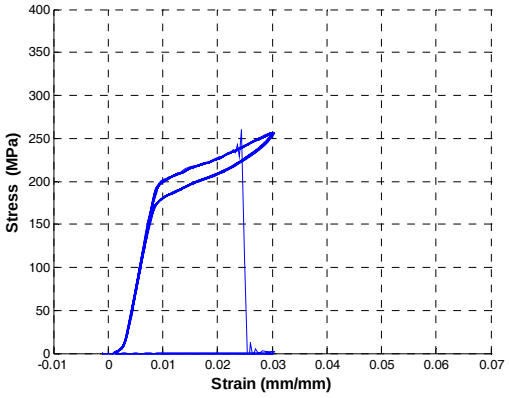

(d) Wire 11b

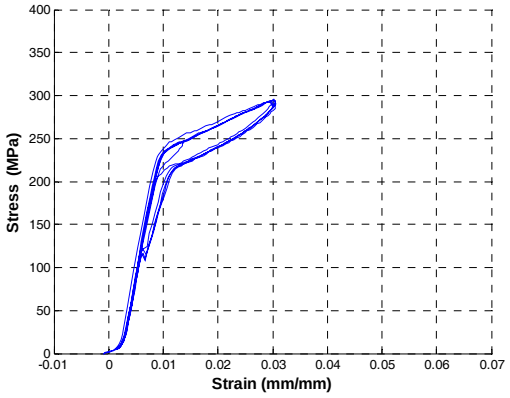

(e) Wire 12a

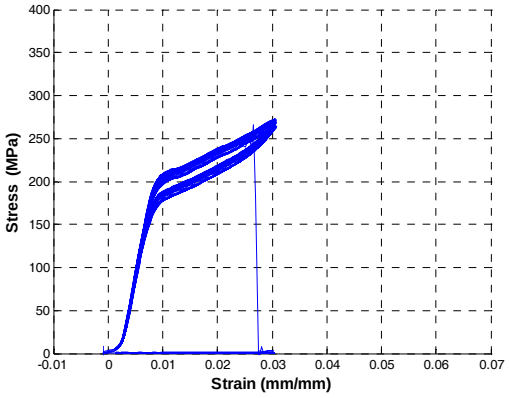

(f) Wire 12b

Figure 33. Results of Cu-Al-Be wires tested on 7/18/2007

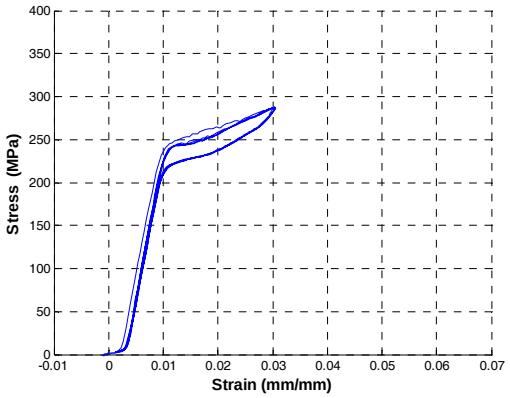

(a) Wire 13a

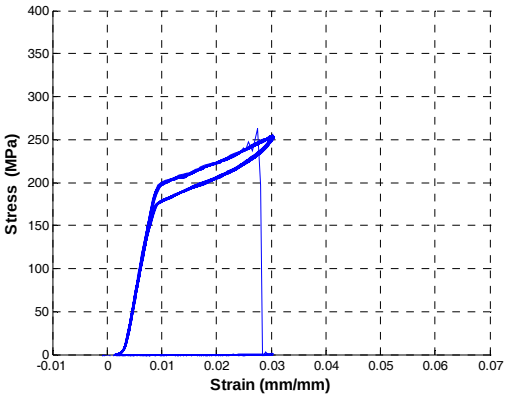

(b) Wire 13b

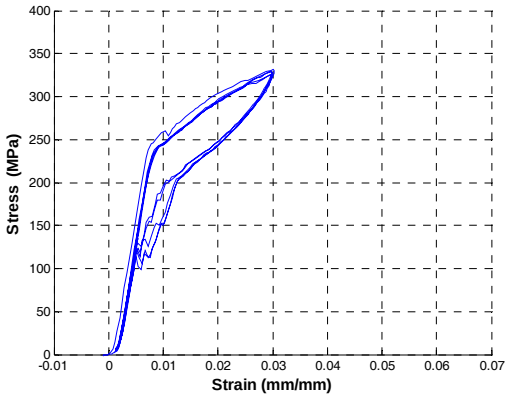

(c) Wire 14a

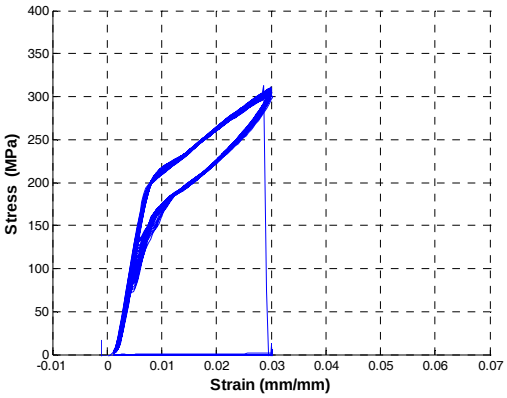

(d) Wire 14b

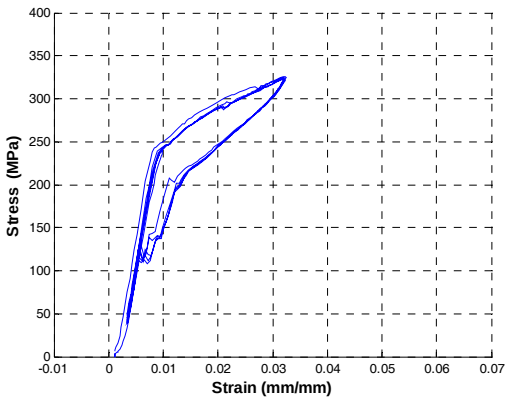

(e) Wire 15a

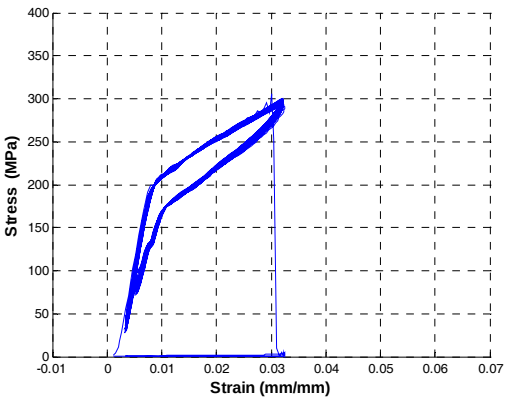

(f) Wire 15b

Figure 34. Results of Cu-Al-Be wires tested on 7/18/2007

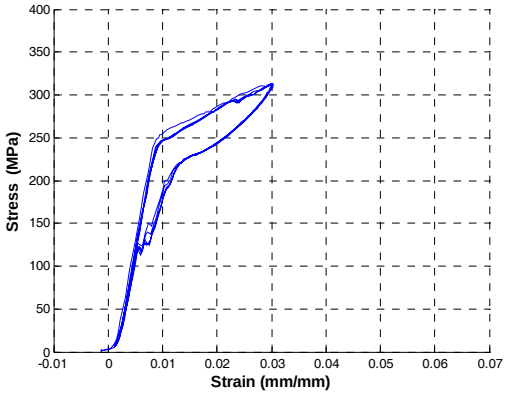

(a) Wire 1a

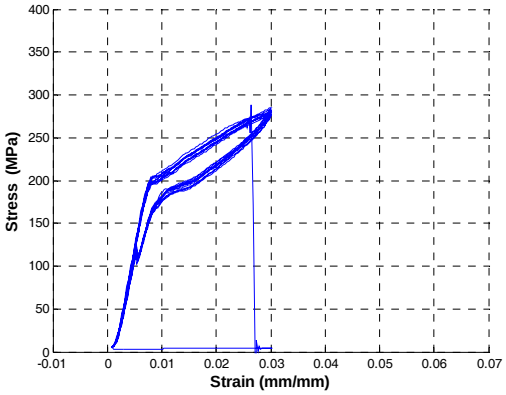

(b) Wire 1b

(c) Wire 2a (not available)

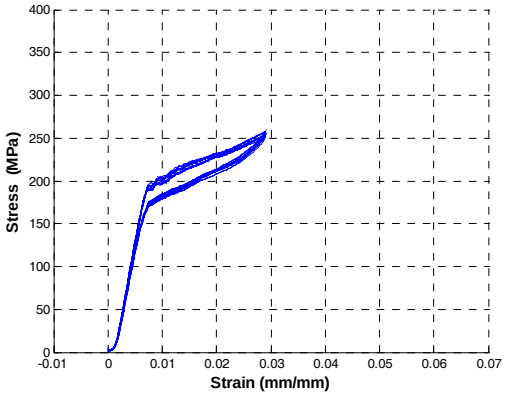

(d) Wire 2b

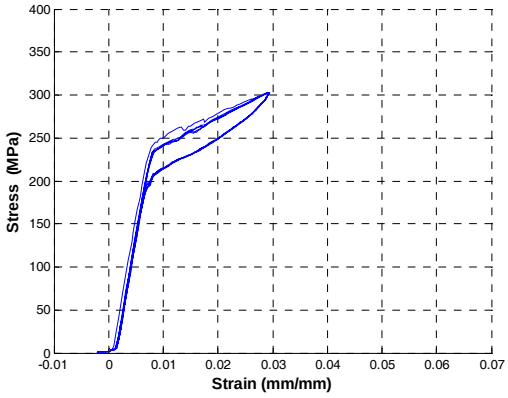

(e) Wire 3a

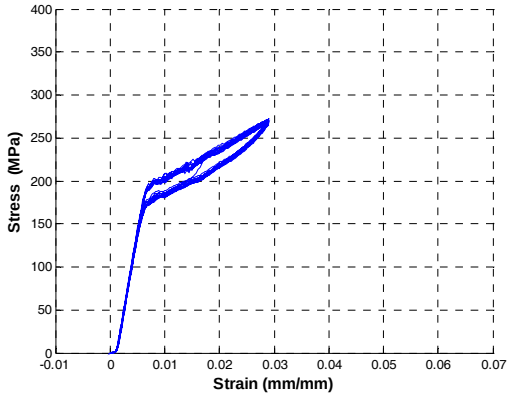

(f) Wire 3b

Figure 35. Results of Cu-Al-Be wires tested on 7/20/2007

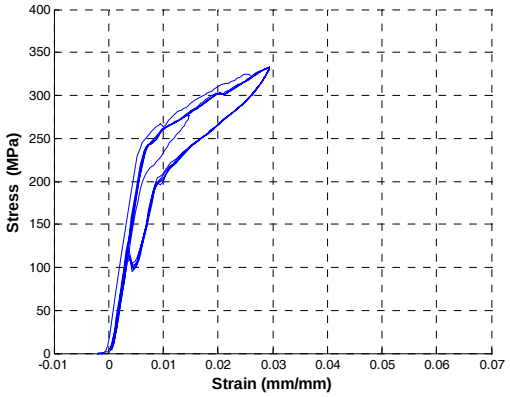

(a) Wire 4a

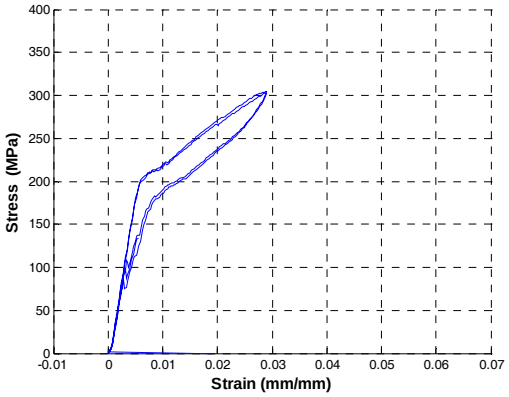

(b) Wire 4b

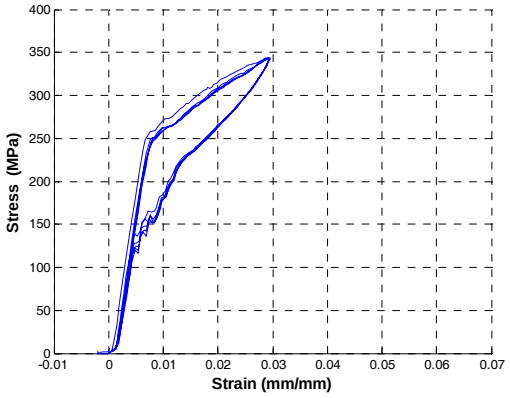

(c) Wire 5a

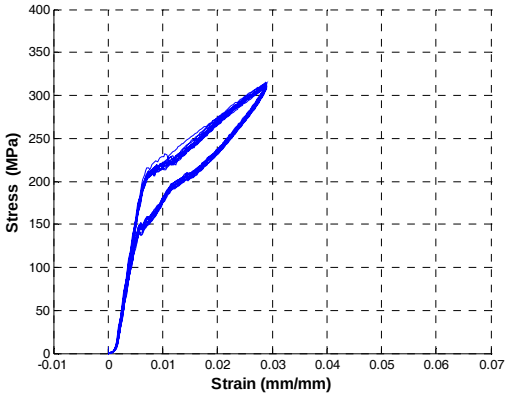

(d) Wire 5b

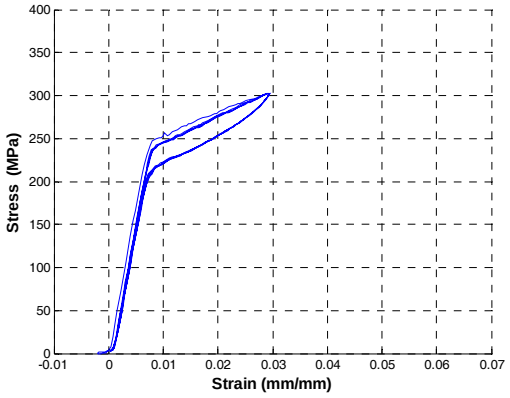

(e) Wire 6a

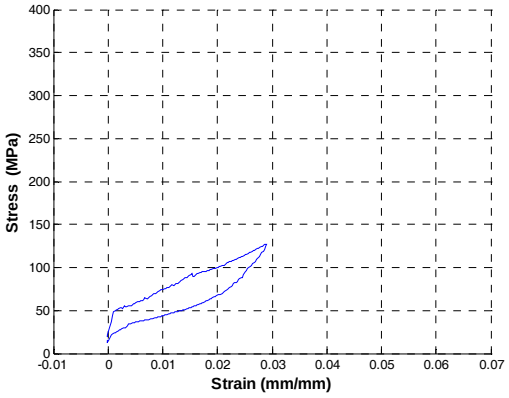

(f) Wire 6b

Figure 36. Results of Cu-Al-Be wires tested on 7/20/2007

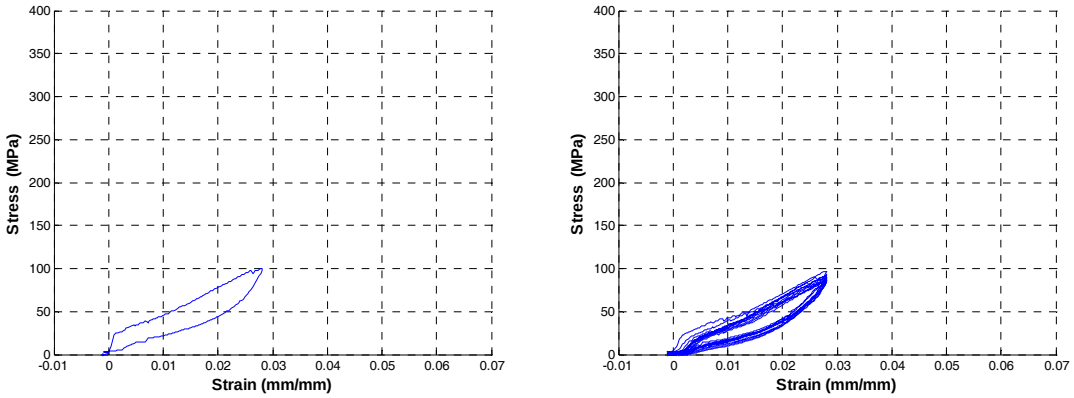

(a) Wire 6a (b) Wire 6d

Figure 37. Results of Cu-Al-Be wires tested on 7/20/2007

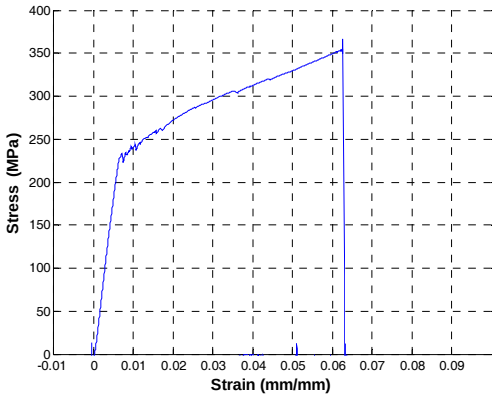

(a) Wire 7

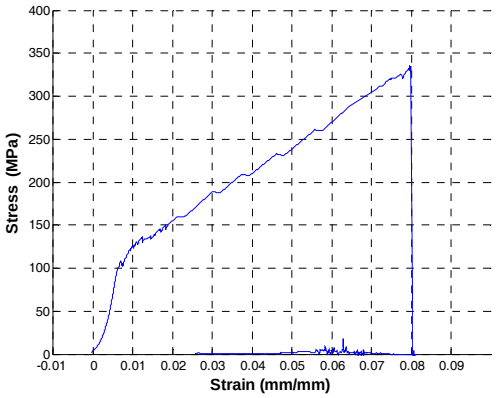

(b) Wire 8

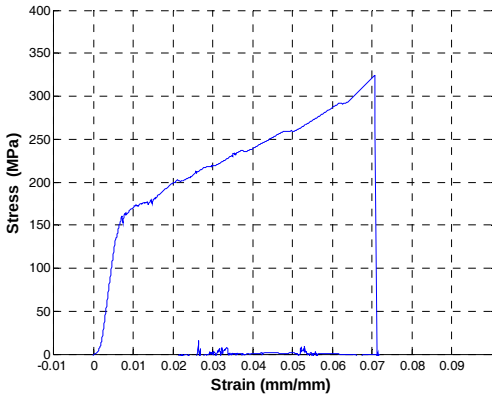

(c) Wire 9

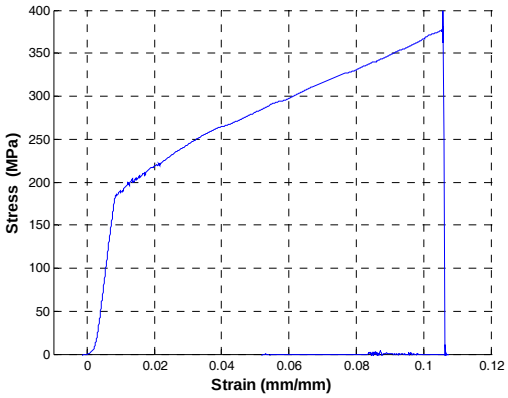

(d) Wire 10

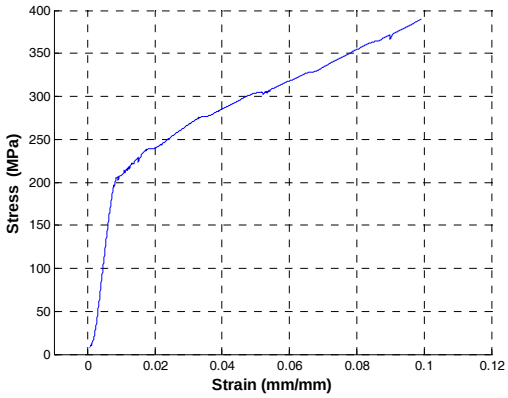

(e) Wire 11

Figure 38. Results of Cu-Al-Be wires tested on 7/20/2007 (monotonic test)

Chapter 4

Conclusions

In this study, uniaxial cyclic tests as well as monotonic tests of superelastic Cu-Al-Be wires were performed at cold temperatures using a temperature chamber. Each Cu-Al-Be wire sample was tested under a particular combination of test temperatures (23ºC, 0ºC - 25ºC, -50ºC), strain rate (0.0012 sec^{-1} or 0.06 sec^{-1}), and heat treatment (batch 1 or batch 2). Therefore, the effects of test temperature, strain rate, and heat treatment on key hysteresis parameters of the Cu-Al-Be wires including transformation stress (i.e., stress of the upper transformation plateau), energy dissipated per cycle (or equivalent damping ratio), elastic modulus, and slope of the upper transformation plateau are studied.

It is found that at cold temperatures the superelastic Cu-Al-Be wires have decreased transformation stress compared to room temperature test results and have longer fatigue life. The transformation stress of the Cu-Al-Be wires being tested increases almost linearly with temperature. The transformation stresses of the Cu-Al-Be wires from two different batches seem to be very close to each other at each test temperature and follow a similar temperature variation pattern. Higher strain rate appear to lead to slightly increased transformation stress level, especially at lower temperatures.

It is seen that for batch 1, the energy dissipation per load cycle does not change with temperature while for batch 2 the energy dissipation at room temperature is considerably greater than that at cold temperatures. For batch 1, the loading rate seems to have no effect on the energy dissipation capacity of Cu-Al-Be wires. For batch 2, at room

temperature, higher loading rate leads to increased energy dissipation while at cold temperatures, loading rate has very little or no effect on the energy dissipation capacity of Cu-Al-Be wires. The elastic modulus of batch 2 wires is slightly higher than that of batch 1 wires. No significant variation pattern of the elastic modulus with respect to temperature and loading rates is observed. Loading rate seems to have very little effect on the upper transformation plateau slope of the Cu-Al-Be wires. It is also seen that with the increase of test temperature the value of upper transformation plateau slope decreases.

It is found that the fatigue life of Cu-Al-Be wires generally decreases with increasing test temperature, apparently due to the increase in transformation stress. Different heat treatment may lead to a significant change in cyclical life of Cu-Al-Be wires. It is seen that batch 1 wires have much higher cyclic life than batch 2 wires.

For the monotonic test, similar observations to those for cyclic loading test can be made. The transformation stress follows the same trend as that of the cyclic loading test, that is, with increasing temperature, the transformation stress increases. The fracture point of Cu-Al-Be under monotonic loading seems to have no correlation with test temperature in any way.

Through this test, it is shown that with proper composition Cu-Al-Be alloy will maintain its superelastic capabilities down to -85ºC, which is approximately the most extreme temperature ever recorded on the earth. Therefore, Cu-Al-Be alloy has a potential to be used re-centerable damping devices at cold temperatures, such as bridge cable restrainers in the winter climates of places like Missouri and Canada.

Acknowledgement

The authors are grateful to the Pennsylvania Infrastructure Technology Alliance and Lehigh University for providing partial financial support for this research project. The second author (J Camilleri) was supported through a summer REU grant from the ATLSS Research Center from May 24 to August 3 2007. However, the opinions and conclusions expressed in this paper are solely those of the writers and do not necessarily reflect the views of the sponsors.

Reference

ASTM 2006 Standard Specification for Structural Steel for Bridges, A 709/A 709M -05, *Annual Book of ASTM Standards* (vol. 01.04), West Conshohocken, Pennsylvania, USA, pg. 372 – 379.

Andrawes B and Des Roches R 2005 Unseating prevention for multiple frame bridges using superelastic devices *Smart Materials Structures* **14** S60–S67

Casciati F and Faravelli L 2004 Experimental characterization of a Cu-based shape memory alloy toward its exploitation in passive control devices *J. Phys. IV* 115 299-306.

Cerda M, Boroschek R, Farías G, Moroni O and Sarrazin M 2006 Shaking table test of a reduced-scale structure with copper-based SMA energy dissipation devices *Proc 8th U.S. National Conference on Earthquake Engineering* April 18-22, 2006, San Francisco, California, USA.

Dicleli M and Bruneau M 1995 Seismic performance of multispan simply supported slab-on-girder steel highway bridges *Engineering Structures* **17**(1) 4–14.

Hsu Y T and Fu C C 2004 Seismic Effect on Highway Bridges in Chi Chi Earthquake *Journal of Performance of Constructed Facilities* **18**(1) 47-53.

Isalgue A, Lovey F C, Terriault P, Martorell F, Torra R M and Torra V 2006 SMA for dampers in civil engineering *Materials Transactions* **47**(3) 682-690.

Julian F D R, Hayashikawa T and Obata T 2007 Seismic performance of isolated curved steel viaducts equipped with deck unseating prevention cable restrainers *Journal of Constructional Steel Research* **63**(2) 237-253

Saiidi M, Randall M, Maragakis E and Isakovic T 2001 Seismic restrainer design methods for simply supported bridges *J. Bridge Engrg.* **6** 307–15